Finite Models for Arithmetical Quantum Chaos

Audrey Terras

Math. Dept., U.C.S.D., San Diego, Ca 92093-0112

Abstract. Physicists have long studied spectra of Schrödinger operators and random matrices thanks to the implications for quantum mechanics. Analogously number theorists and geometers have investigated the statistics of spectra of Laplacians on Riemannian manifolds. This has been termed by Sarnak "arithmetic quantum chaos" when the manifolds are quotients of a symmetric space modulo an arithmetic group such as the modular group $SL(2,\mathbb{Z})$. Equivalently one seeks the statistics of the zeros of Selberg zeta functions. Parallels with the statistics of the zeros of the Riemann zeta function have been evident to physicists for some time. Here we survey what may be called "finite quantum chaos" seeking connections with the continuous theory. We will also discuss discrete analogue of Selberg's trace formula as well as Ihara zeta functions of graphs.

Part 1

Lecture 1. Finite Models

1. Introduction

This is a story of a tree related to the spectral theory of operators on Hilbert spaces. The tree has three branches as in Figure 1. The left branch is that of quantum physics: the statistics of energy levels of quantum mechanical systems; i.e. the eigenvalues of the Schrödinger operator $\mathcal{L}\phi_n = \lambda_n\phi_n$. The middle branch is that of geometry and number theory. In the middle we see the spectrum of the Laplace operator $\mathcal{L} = \Delta$ on a Riemannian manifold M such as the fundamental domain of the modular group $SL(2,\mathbb{Z})$ of 2×2 integer matrices with determinant 1. This is an example of what Peter Sarnak has called "arithmetic quantum chaos." The right branch is that of graph theory: the statistics of the spectrum of $\mathcal{L} =$ the adjacency operator (or combinatorial Laplacian) of a Cayley graph of a finite matrix group. We call this subject "finite quantum chaos."

What about the roots of the tree? These roots represent zeta functions and trace formulas. On the left is the Gutzwiller trace formula. In the middle is the Selberg trace formula and the Selberg zeta function. On the right is the Ihara zeta function of a finite graph and discrete analogues of the Selberg trace formula. The zeros of the zeta functions correspond sometimes mysteriously to the eigenvalues of the operators at the top of the tree.

Here we will emphasize the right branch and root of the tree. But we will discuss the connections with the other tree parts. The articles [**84**], [**85**], [**86**] are closely related to these lectures. A good website for quantum chaos is that of Matthew W. Watkins www.maths.ex.ac.uk/~mwatkins.

We quote Oriol Bohigas and Marie-Joya Gionnoni [**11**], p. 14: "The question now is to discover the stochastic laws governing sequences having very different origins, as illustrated in ... [Figure 2]. There are displayed six spectra, each containing 50 levels ..." Note that the spectra have been rescaled to the same vertical axis from 0 to 49.

In Figure 2, column (a) represents a Poisson spectrum, meaning that of a random variable with spacings of probability density e^{-x}. Column (b) represents primes between 7791097 and 7791877. Column (c) represents the resonance energies of the compound nucleus observed in the reaction $n+{}^{166}Er$. Column (d) comes from eigenvalues corresponding to transverse vibrations of a membrane whose boundary is the Sinai billiard which is a square with a circular hole cut out centered at the center of the square. Column (e) is from the positive imaginary parts of zero's of the Riemann zeta function (from the 1551th to the 1600th zero). Column (f) is equally spaced - the picket fence or uniform distribution. Column (g) comes from Sarnak [**67**] and corresponds to eigenvalues of the Poincaré Laplacian on the fundamental domain of the modular group $SL(2,\mathbb{Z})$ consisting of 2×2 integer matrices of determinant 1. From the point of view of randomness, columns (g) and (h) should be moved to lie next to column (b). Column (h) is the spectrum of a finite upper half plane graph for p=53 ($a = \delta = 2$), without multiplicity.

Exercise 1. *Produce your own versions of as many columns of Figure 2 as possible. Also make a column for level spacings of lengths of primitive closed geodesics in $SL(2,\mathbb{Z})\backslash H$. See pages 277-280 of Terras* [**83**]*, Vol. I.*

Given some favorite operator $\mathcal{L}$ acting on some Hilbert space $L^2(M)$, as in the first paragraph of this section, one has favorite questions in quantum chaos theory

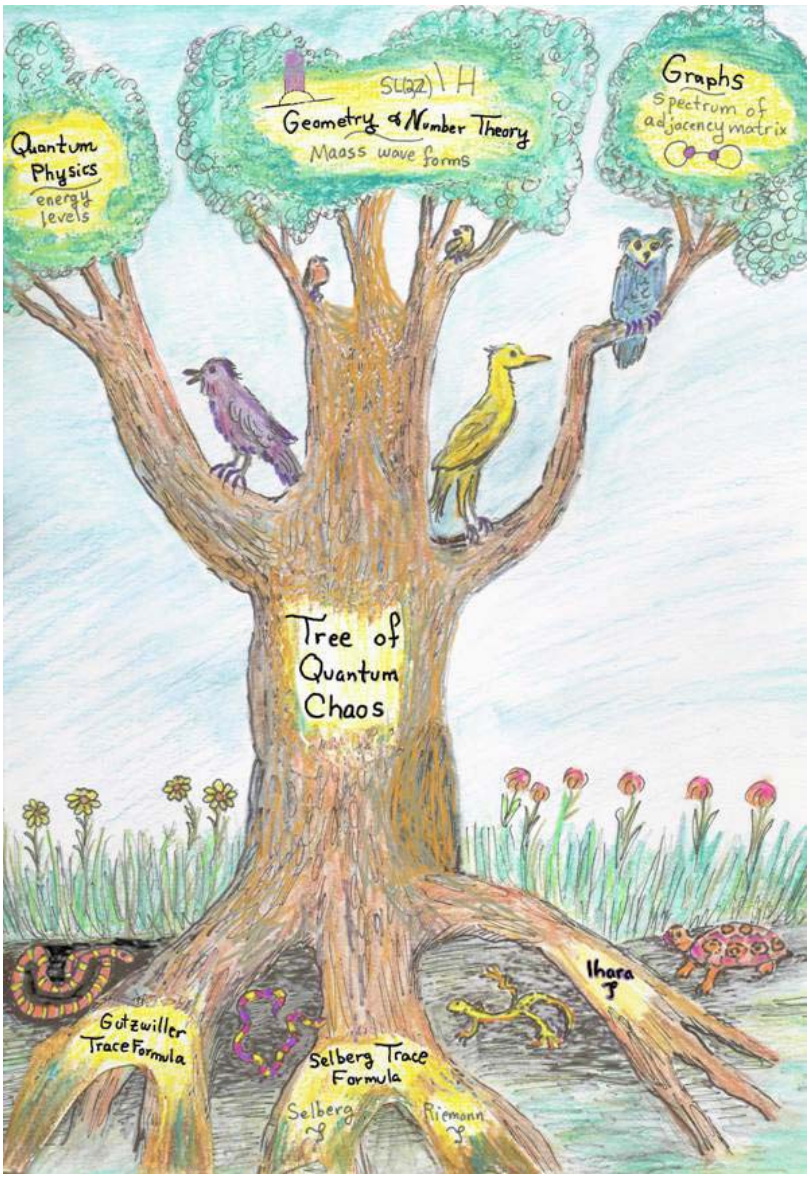

FIGURE 1. The Tree of Quantum Chaos

(see Sarnak [**67**] or Hejhal et al [**37**] or the talks given in the spring, 1999 random matrix theory workshop at the web site http://www.msri.org).

Examples of Questions of Interest

- 1) Does the spectrum of $\mathcal{L}$ determine M? Can you hear the shape of M?
- 2) Give bounds on the spectrum of $\mathcal{L}$.
- 3) Is the histogram of the spectrum of $\mathcal{L}$ given by the Wigner semi-circle distribution [**91**]?

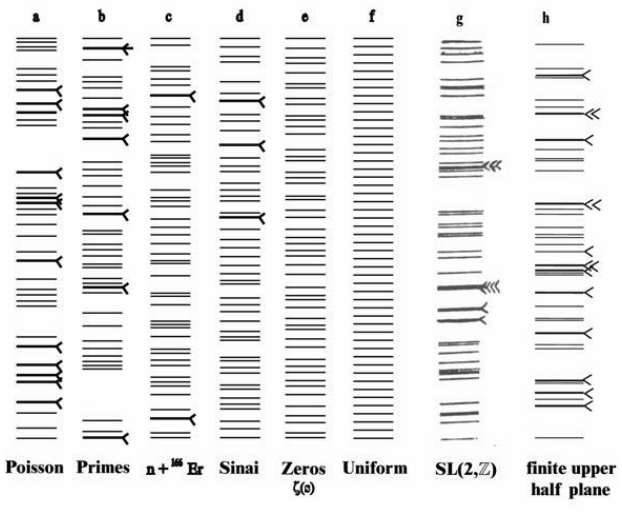

FIGURE 2. Columns (a)-(f) are from Bohigas and Giannoni [**11**] and column (g) is from Sarnak [**67**]. Segments of "spectra," each containing 50 levels. The "arrowheads" mark the occurrence of pairs of levels with spacings smaller than 1/4. The labels are explained in the text. Column (h) contains finite upper half plane graph eigenvalues (without multiplicity) for the prime 53, with $\delta = a = 2$.

- 4) Arrange the spectrum of $\mathcal{L}$ so that $\lambda_n \leq \lambda_{n+1}$. Consider the level spacings $|\lambda_{n+1} - \lambda_n|$ normalized to have mean 1. What is the histogram for the level spacings?
- 5) Behavior of the nodal lines ($\phi_n = 0$) of eigenfunctions of $\mathcal{L}$ as $n \to \infty$.

Note that when M is finite, we will consider a sequence M_j such that $m_j = |M_j| \to \infty$ as $j \to \infty$ and we seek limiting distributions of spectra and level spacings as $j \to \infty$. Now the $\phi_n = (f_1^{(n)}, ..., f_m^{(n)})$ are eigenvectors of the matrix $\mathcal{L}_j$ acting on the finite dimensional Hilbert space $\mathbb{C}^{m_j} \cong L^2(M_j)$ and we study the limiting behavior of the set of indices j for which $f_j^{(n)} = 0$.

The trace formula is the main tool in answering such questions. We will compare three sorts of trace formulas in Lecture 2.

I would like to thank Stefan Erickson and Derek Newland for help with the proof reading of this article.

2. Quantum Mechanics.

Quantum mechanics says the energy levels E of a physical system are the eigenvalues of a Schrödinger equation $H\phi = E\phi$, where H is the Hamiltonian (a differential operator), ϕ is the state function (eigenfunction of H), and E is the energy level (eigenvalue of H). For complicated systems, physicists decided that it would usually be impossible to know all the energy levels. So they investigate the statistical theory of these energy levels. This sort of thing happens in ordinary

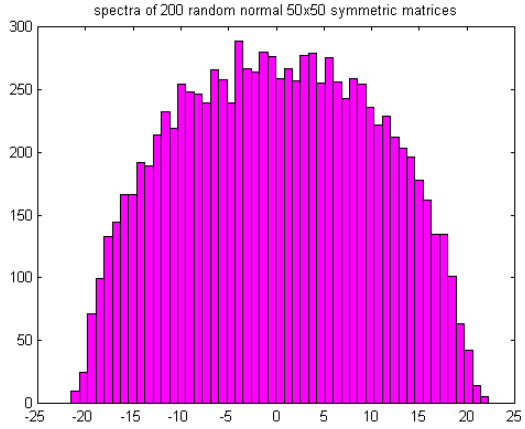

FIGURE 3. Histogram of the spectra of 200 random real 50x50 symmetric matrices created using Matlab.

statistical mechanics as well. Of course symmetry groups (i.e., groups of motions commuting with H) have a big effect on the energy levels.

In the 1950's, Wigner (see [**91**]) said why not model H with a large real symmetric $n \times n$ matrices whose entries are independent Gaussian random variables. He found that the histogram of the eigenvalues looks like a semi-circle (or, more precisely, a semi-ellipse). For example, he considered the eigenvalues of 197 "random" real symmetric 20x20 matrices. Figure 3 below shows the results of an analogue of Wigner's experiment using Matlab. We take 200 random real symmetric 50x50 matrices with entries that are chosen according to the normal distribution. Wigner notes on p. 5: "What is distressing about this distribution is that it shows no similarity to the observed distribution in spectra." However, we will find the semi-circle distribution is a very common one in number theory and graph theory. See Figures 7 and 9, for example. In fact, number theorists have a different name for it - the Sato-Tate distribution. It appears as the limiting distribution of the spectra of k-regular graphs as the number of vertices approaches infinity under certain hypotheses (see McKay [**58**]).

EXERCISE 2. *Repeat the experiment that produced Figure 1 using uniformly distributed matrices rather than normally distributed ones. This is a problem best done with Matlab which has commands rand(50) and randn(50) giving a random and a normal random* 50×50 *matrix, respectively.*

So physicists have devoted more attention to histograms of level spacings rather than levels. This means that you arrange the energy levels (eigenvalues) E_i in decreasing order:

$$E_1 \geq E_2 \geq \cdots \geq E_n.$$

Assume that the eigenvalues are normalized so that the mean of the level spacings $|E_i - E_{i+1}|$ is 1. Then one can ask for the shape of the histogram of the normalized level spacings. There are (see Sarnak [**67**]) two main sorts of answers to this question: Poisson, meaning e^{-x}, and GOE (see Mehta [**59**]) which is more complicated

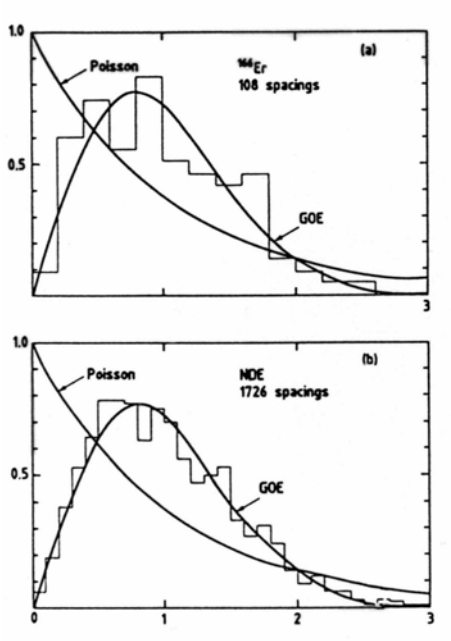

FIGURE 4. (from Bohigas, Haq, and Pandey [**12**]) Level spacing histogram for (a) ^{166}Er and (b) a nuclear data ensemble.

to describe exactly but looks like $\frac{\pi}{2}xe^{-\frac{\pi x^2}{4}}$ (the Wigner surmise). Wigner (see [**91**]) conjectured in 1957 that the level spacing histogram for levels having the same values of all quantum numbers is given by $\frac{\pi}{2}xe^{-\frac{\pi x^2}{4}}$ if the mean spacing is 1. In 1960, Gaudin and Mehta found the correct distribution function which is surprisingly close to Wigner's conjecture but different. The correct graph is labeled GOE in Figure 4. Note the level repulsion indicated by the vanishing of the function at the origin. Also in figure 4, we see the Poisson density which is e^{-x}.

See the next section for more information on the Gaudin-Mehta distribution. You can find a Mathematica program to compute this function at the website in [**30**]. Sarnak [**67**], p. 160 says: "It is now believed that for integrable systems the eigenvalues follow the Poisson behavior while for chaotic systems they follow the GOE distribution." Here GOE stands for Gaussian Orthogonal Ensemble - the eigenvalues of a random $n \times n$ symmetric real matrix as n goes to infinity. And GUE stands for the Gaussian Unitary Ensemble (the eigenvalues of a random $n \times n$ Hermitian matrix).

There are many experimental studies comparing GOE prediction and nuclear data. Work on atomic spectra and spectra of molecules also exists. In Figure 4, we reprint a figure of Bohigas, Haq, and Pandey [**12**] giving a comparison of histograms of level spacings for (a) ^{166}Er and (b) a nuclear data ensemble (or NDE) consisting of about 1700 energy levels corresponding to 36 sequences of 32 different nuclei. Bohigas et al say: "The criterion for inclusion in the NDE is that the individual sequences be in general agreement with GOE."

More references for quantum chaos are F. Haake [**33**] and Z. Rudnick [**65**].

3. Arithmetic Quantum Chaos.

Here we give a sketch of the subject termed "arithmetic quantum chaos" by Sarnak [**67**]. A more detailed treatment can be found in Katz and Sarnak [**44**], [**45**], Sarnak [**67**]. See Cipra [**22**], pp. 20-35 for a very accessible introduction. Another reference is the volume [**37**]. The MSRI website (net address: http://www.msri.org/) has movies and transparencies of many talks from 1999 on the subject. See, for example, the talks of Sarnak from Spring, 1999. Cipra, loc. cit., p. 25 says: "Roughly speaking, quantum chaos is concerned with the spectrum of a quantum system when the classical version of the system is chaotic." The arithmetic version of the subject involves objects of interest to number theorists which may or may not be known to be related to eigenvalues of operators. The first such objects are zeros of zeta functions. The second are eigenvalues of Laplacians on quotients of arithmetic groups.

3.1. Zeros of Zeta Functions of Number Theory. Andrew Odlyzko has created pictures of the level spacing distribution for the non-trivial zeros of the **Riemann zeta function** defined as follows, for $Re(s) > 1$,

$$\zeta(s) = \sum_{n \geq 1} n^{-s} = \prod_{p \text{ prime}} \left(1 - \frac{1}{p^s}\right)^{-1}.$$

See Odlyzko's joint work with Forrester [**30**] or see

www.dtc.umn.edu/~odlyzko/doc/zeta.html).

Riemann showed how to do the analytic continuation of zeta to $s \in \mathbb{C}$ with a pole at $s = 1$. Thanks to Hadamard factorization, the statistics of the zeros of $\zeta(s)$ are intimately connected with the statistics of the primes. A modicum of knowledge about the zeros of zeta led to the proof by Hadamard and de la Vallée Poussin of the **prime number theorem**, saying that the number of primes less than or equal to x is asymptotic to $x/logx$, as x goes to infinity.

Riemann hypothesized that the non-real zeros of zeta are on the line $Re(s) = 1/2$. If you know a proof, you are about to be a millionaire (see the web site www.claymath.org). The hypothesis has been checked for the lowest 100 billion zeros (see the web site www.hipilib.de/zeta/index.html). Assume the Riemann hypothesis and look at the zeros ordered by imaginary part

$$\left\{ \gamma_n \,\middle|\, \zeta(\frac{1}{2} + i\gamma_n) = 0,\ \gamma_n > 0 \right\}.$$

For the normalized level spacings, replace γ_n by $\widetilde{\gamma_n} = \frac{1}{2\pi}\gamma_n log\,\gamma_n$, since we want the mean spacing to be one. Here one needs to know that the number of γ_n such that $\gamma_n \leq T$ is asymptotic to $\frac{1}{2\pi}T\log T$ as $T \longrightarrow \infty$.

Historically the connections between the statistics of the Riemann zeta zeros γ_n and the statistics of the energy levels of quantum systems were made in a dialogue of Dyson and H. Montgomery over tea at the Institute for Advanced Study, Princeton. Odlyzko's experimental results show that the level spacings $|\gamma_n - \gamma_{n+1}|$, for large n, look like that of the Gaussian unitary ensemble (GUE). See Figure 5.

Note. The level spacing distribution for the eigenvalues of Gaussian unitary matrices is not a standard function in Matlab, Maple or Mathematica. Sarnak [**67**] and Katz and Sarnak [**45**] proceed as follows. Let $K_s : L^2[0,1] \longrightarrow L^2[0,1]$ be the integral operator with kernel defined by

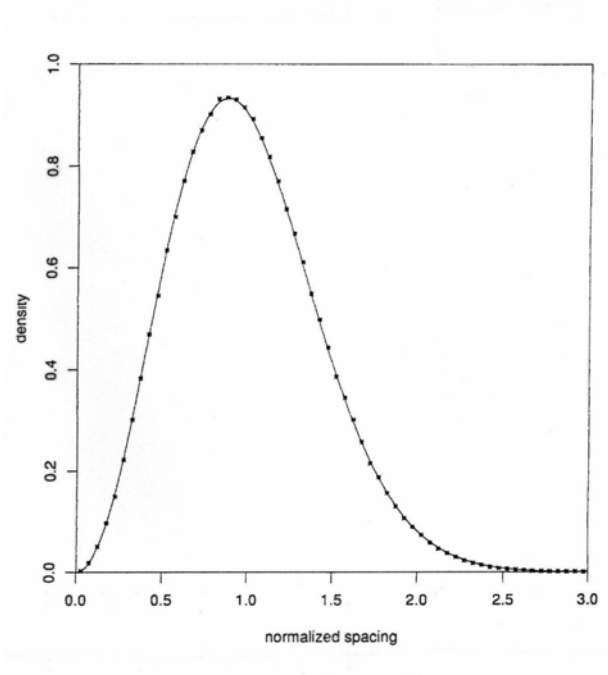

FIGURE 5. From Cipra [**22**]. Odlyzko's comparison of level spacing of zeros of the Riemann zeta function and that for GUE (Gaussian unitary ensemble). See Odlyzko and Forrester [**30**]. The fit is good for the 1,041,000 zeros near the 2×10^{20} zero.

$$h_s(x,y) = \frac{sin\left(\frac{\pi s(x-y)}{2}\right)}{\frac{\pi(x-y)}{2}}, \text{ for } \quad s \geq 0.$$

Approximations to this kernel have been investigated in connection with the uncertainty principle (see Terras [**83**], Vol. I, p. 51). The eigenfunctions are spheroidal wave functions. Let $E(s)$ be the Fredholm determinant $det(I - K_s)$ and let $p(s) = E''(s)$. Then $p(s) \geq 0$ and $\int_0^\infty p(s)ds = 1$. The Gaudin-Mehta distribution ν is defined in the GUE case by $\nu(I) = \int_I p(s)ds$. For the GOE case the kernel h_s is replaced by $\{h_s(x,y) + h_s(-x,y)\}/2$. See also Mehta [**59**].

Katz and Sarnak [**44**], [**45**] have investigated many zeta and L-functions of number theory and have found that "the distribution of the high zeroes of any L-function follow the universal GUE Laws, while the distribution of the low-lying zeros of certain families follow the laws dictated by symmetries associated with the family. The function field analogues of these phenomena can be established..." More precisely, they show that "the zeta functions of almost all curves C [over a finite field $\mathbb{F}_q$] satisfy the Montgomery-Odlyzko law [GUE] as q and g [the genus] go to infinity." However, not a single example of a curve with GUE zeta zeros has ever been found.

These statistical phenomena are as yet unproved for most of the zeta functions of number theory; e.g., Riemann's. But the experimental evidence of Rubinstein

[**64**] and Strömbergsson [**79**] and others is strong. Figures 3 and 4 of Katz and Sarnak [**45**] show the level spacings for the zeros of the L-function corresponding to the modular form Δ and the L-function corresponding to a certain elliptic curve. Strömbergsson's web site has similar pictures for L-functions corresponding to Maass wave forms (http://www.math.uu.se/~andreas/zeros.html). All these pictures look GUE.

3.2. Eigenvalues of the Laplacian on Riemannian Manifolds M. References for this subject include [**16**], [**37**], [**66**], [**67**], [**83**]. Suppose for concreteness that $M = \Gamma\backslash H$, where H denotes the Poincaré upper half plane and Γ is a discrete group of fractional linear transformations $z \longrightarrow \frac{az+b}{cz+d}$, for a, b, c, d real with $ad-bc = 1$. Then one is interested in the square-integrable functions ϕ on M which are eigenfunctions of the Poincaré Laplacian; i.e.,

$$\Delta\phi = y^2\left(\frac{\partial^2\phi}{\partial x^2} + \frac{\partial^2\phi}{\partial y^2}\right) = \lambda\phi. \tag{3.1}$$

The most familiar example of an arithmetic group is $SL(2,\mathbb{Z})$, the **modular group** of 2×2 integer matrices of determinant one. A function ϕ which is Γ-invariant, satisfies (3.1), and is square integrable on M is a **Maass cusp form**. The λ's form the discrete spectrum of Δ. Studies have been made of level spacings of the eigenvalues λ. The zeta function that is involved is the Selberg zeta function (defined in Table 3 of Lecture 2). Its non-trivial zeros correspond to these eigenvalues.

Because M is not compact for the modular group, there is also a continuous spectrum (the Eisenstein series). This makes it far more difficult to do numerical computations of the discrete spectrum. See Terras [**83**], Vol. I, p. 224, for some history of early numerical blunders. Other references are Elstrodt [**25**] and Hejhal [**36**]. Equivalently one can replace the Poincaré upper half plane with the Poincaré unit disk.

I like to say that an arithmetic group is one in which the integers are lurking around in its definition. Perhaps a number theorist ought to be able to smell them.

If you really must be precise about it, you should look at the articles of Borel [**14**], p. 20. First you need to know that 2 subgroups A, B of a group C are said to be **commensurable** iff $A \cap B$ has finite index in both A and B. Then suppose Γ is a subgroup an algebraic group G over the rationals as in Borel [**14**], p. 3. One says that Γ is **arithmetic** if there is a faithful rational representation (see Borel [**14**], p. 6) $\rho : G \to GL(n)$, the general linear group of $n \times n$ non-singular matrices, such that ρ is defined over $\mathbb{Q}$ and such that $\rho(\Gamma)$ is commensurable with $\rho(\Gamma) \cap GL(n,\mathbb{Z})$. Arithmetic and non-arithmetic subgroups of $SL(2,\mathbb{C})$ are discussed by Elstrodt, Grunewald, and Mennicke in [**26**], Chapter 10.

The top of Figure 6 shows the fundamental domain of an arithmetic group in the unit disk. Note that the upper half plane can be identified with the unit disc via the map sending z in H to $\frac{z-i}{z+i}$. C. Schmit [**68**] found 1500 eigenvalues for the Dirichlet problem of the Poincaré Laplacian on the triangle OLM with angles $\pi/8, \pi/2, \pi/3$. The histogram of level spacings for this problem is the lower right part of Figure 6. Schmit also considered the Dirichlet problem for a non-arithmetic triangle with angles $\pi/8, \pi/2, 67\pi/200$. The level spacing histogram for this non-arithmetic triangle is given in the lower left of Figure 6. Schmit concludes: "The spectrum of the tessellating [arithmetic] triangle exhibits neither level repulsion nor spectral rigidity and there are strong evidences that asymptotically the spectrum is

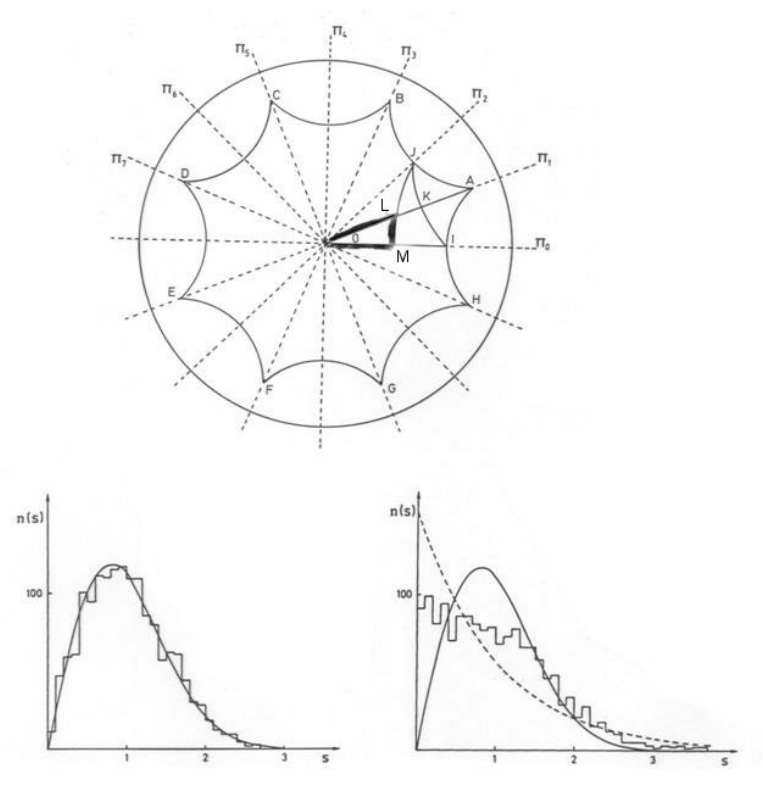

FIGURE 6. From Schmit [**68**]. The top shows the fundamental domain of an arithmetic group which tessellates the Poincare disk. The lower right shows the level spacing histogram for the Dirichlet problem on the triangle OLM using the 1500 eigenvalues computed by Schmit using the method of collocation. The lower left is the analogous histogram for a non-arithmetic triangle. The solid line is the GOE distribution and the dashed one is Poisson (e^{-x}).

of Poisson type, although the billiard is known to be a strongly chaotic system. The spectrum of the non-tessellating [non-arithmetic] triangle, whose classical properties are not known but which is probably a chaotic system too, exhibits the essential features of a generic chaotic system, namely the level repulsion and the spectral rigidity of GOE, as already observed in other chaotic systems."

Steil (in Hejhal [**37**], pp. 617-641) performs analogous experiments to those of Schmit for arithmetic subgroups of $SL(2,\mathbb{C})$ acting on three-dimensional quaternionic upper half space. Once more he found a Poisson level spacing. He says: "one is tempted to regard this as a universal feature of arithmetic systems."

4. Graph Theory.

The spectrum of a partial differential operator like the Schrödinger operator above (or the Laplace operator on a Riemann surface) is a topic in linear algebra on infinite dimensional vector spaces; i.e., functional analysis. This subject is much

harder than the finite dimensional version. So, like S. Wolfram with his cellular automata, let us replace the continuous, calculus-oriented subject, with a finite computer-friendly subject. It is clearly much easier to experiment with the finite quantum chaos statistics. One does not need a supercomputer!

So we replace the differential operator with a finite analogue - the adjacency matrix/operator of a graph. Think of a graph as a system of masses connected by springs or rubber bands. This is a reasonable model for a molecule. See Starzak [**77**]. Here we consider only Cayley graphs of groups for which we understand the representations. This will be a big help in computing the eigenvalues/energy levels since by a result in the first chapter or so of a book on group representations, the adjacency operation of a Cayley graph of a group G is block diagonalized by the Fourier transform on G. See [**82**], pp. 256-7, 284.

The spectral theory of graphs has a long history in its own right. See Biggs [**10**] and Cvetković, Doob and Sachs [**23**] as well as the more recent book of Fan Chung [**20**]. Much of the motivation comes from quantum chemistry as well as physics, mechanical engineering, and computer science. One would also expect that there should be more applications in areas such as numerical analysis for problems with symmetry. Hückel's theory in chemistry seeks to study such things as the stability of a molecule by computing a constant from the eigenvalues of A for the graph associated to the molecule. One very interesting example was provided recently by the work of Chung and Sternberg [**21**] on the application of the representation theory of the icosahedral group to explain the spectral lines of the buckyball C_{60}. They find that the stability constant for the buckyball is greater than that for benzene. See also Chung [**20**] and Sternberg [**78**].

Most of spectral graph theory is not really concerned with finding histograms such as Figures 7 and 8, but instead with more basic questions such as 2b) below. I will assume that our graph X is connected finite and k-regular with adjacency matrix A. Here "k-regular" means that each vertex has k edges coming out.

Now we can re-interpret the 5 questions at the end of section 1 when M is a finite connected regular graph. As we said, for most questions below, we will need an infinite sequence of graphs X_j with $|X_j| \to \infty$, as $j \to \infty$. We assume X_j has adjacency matrix A_j. In question 2b) a graph X is "bipartite" if $X = A \cup B$, where $A \cap B = \emptyset$ such that any edge connects a vertex in A to a vertex in B.

Basic Questions about Spectra of Finite Connected k-Regular Graphs

- 1) Can non-isomorphic graphs have the same spectrum? Can you hear the shape of a graph?
- 2) a) What are bounds on the spectrum of A? Note that k is always an eigenvalue of multiplicity 1. And $-k$ is an eigenvalue iff X is bipartite. Are there gaps in the spectrum or does it approach the interval $[-k, k]$ as the number of vertices of the graph goes to infinity? Is 0 an eigenvalue of A?

  b) What does the size of the second largest eigenvalue of A in absolute value have to do with graph-theoretic constants such as diameter, girth, chromatic number, expansion constants?
- 3) Does the histogram of the spectrum of A_j (the adjacency matrix of X_j) approach the Wigner semi-circle distribution for a sequence of graphs X_j, with $|X_j| \to \infty$, as $j \to \infty$?

- 4) Arrange the spectrum $\{\lambda_n\}$of A_j so that $\lambda_n \leq \lambda_{n+1}$. Consider the level spacings $|\lambda_{n+1} - \lambda_n|$ normalized to have mean 1. What is the limiting histogram for the level spacings as $j \to \infty$?
- 5) What can be said about the behavior of the eigenfunctions (eigenvectors) of A?

Here we will discuss some of these questions for some special types of graphs.

EXERCISE 3. *Show that for a connected k-regular graph X, the degree k is always an eigenvalue of multiplicity 1. Prove that $-k$ is an eigenvalue iff X is bipartite. Figure out the definitions of diameter, girth, chromatic number, expansion constant of a graph and explore the connections with bounds on the second largest eigenvalue of A in absolute value. References are: Biggs* [**10**] *, Bollobas* [**13**]*, Terras* [**82**]*.*

It was shown by Alon and Boppana (see Lubotzky [**52**], p. 57 or Feng and Li [**28**] for a generalization to hypergraphs) that for connected k-regular graphs X, if $\lambda(X)$ denotes the second largest eigenvalue of A in absolute value, then

$$liminf\ \lambda(X) \geq 2(k-1)^{1/2},\ \text{as}\ |X| \longrightarrow \infty.$$

Following Lubotzky, Phillips and Sarnak [**53**], we call a k-regular graph X **Ramanujan** iff

$$\lambda(X) \leq 2(k-1)^{1/2}. \tag{4.1}$$

Thus Ramanujan graphs are the connected k-regular graphs with the smallest possible asymptotic bound on their eigenvalues. Such graphs are good expanders and (when the graph is not bipartite) the standard random walk on X converges extremely rapidly to uniform. This means that Ramanujan graphs make efficient communications networks. See Lubotzky [**52**], Sarnak [**66**], and Terras [**82**]. Finally Ramanujan graphs are those for which the Ihara zeta function satisfies the analogue of the Riemann hypothesis. See Exercise 9 in Lecture 2.

REMARK 1. *The name "Ramanujan" was attached to these graphs by Lubotzky, Phillips and Sarnak* [**53**] *because they needed to use the (now proved) Ramanujan conjecture on the size of Fourier coefficients of modular forms such as Δ in order to show that the graphs they created did satisfy the inequality (4.1).*

Margulis as well as Lubotzky, Phillips and Sarnak [**53**] construct examples of infinite families of Ramanujan graphs of fixed degree. See also Morgenstern [**61**]. There are also examples such as the graphs of Winnie Li [**49**] and the Euclidean and finite upper half plane graphs in Terras [**81**] and [**82**] (see the discussion of Figures 7, 8 and 9 below) which are Ramanujan but the degree increases as the number of vertices increases. Jakobson et al (in [**37**], pages 317-327) studied the eigenvalues of adjacency matrices of generic k-regular graphs and found the level spacing distribution looks GOE as the number of vertices goes to infinity. Their results are purely experimental.

Since Lubotzky, Phillips and Sarnak [**53**] or even earlier, it has been of interest to look at Cayley graphs associated with groups like $GL(2, F)$, the general linear group of 2×2 invertible matrices with entries in F, where F is a finite field or ring. Subgroups like $SL(2, F)$, the special linear group of determinant 1 matrices in $GL(2, F)$, are also important. These groups are useful thanks to the connection with

modular forms - making it possible to use some highly non-trivial number theory to prove that the graphs of interest are Ramanujan, for example. See Lubotzky [**52**] and Sarnak [**66**]. Other references are Chung [**20**], Friedman [**31**], and Li [**49**].

A **Cayley graph** of a finite group G with edge set $S \subset G$ will be denoted $X = X(G, S)$. X has as vertex set the elements of G and edges connect $x \in G$ to xs for all $s \in S$. Normally we assume that S is "symmetric" meaning that $s \in S$ implies $s^{-1} \in S$. This allows us to consider X to be an undirected graph. If S generates G then X is connected. Usually we assume the identity element of G is not in S so that X will not have loops.

If G is the cyclic group $\mathbb{Z}/n\mathbb{Z}$, it is easy to see that a complete orthogonal set of eigenfunctions of A are the characters of G. The characters are $\chi_a(x) = e^{2\pi iax/n}$, for $a \in \mathbb{Z}/n\mathbb{Z}$. The corresponding eigenvalues are $\lambda_a = \sum_{s \in S} \chi_a(s)$. The same formula works for any finite abelian group. When the group is not abelian, things become more complicated. See Terras [**82**].

Histograms of spectra or of level spacings were not considered until later, but Lafferty and Rockmore [**48**] (and in [**31**], pp. 63-73) consider spectral plots that show spectral gaps. In [**37**], pp. 373-386, Lafferty and Rockmore investigate level spacing histograms. They found on page 379, for example, that the cumulative distribution for the level spacings of ten 4-regular graphs on 2,000 vertices generated by running a Markov chain for 10^8 steps looks remarkably close to the cumulative distribution function for the Wigner surmise $1 - exp\left(\frac{-\pi x^2}{4}\right)$. And in Lafferty and Rockmore in [**37**], p. 380, they found that the cumulative distribution function for eigenvalue spacings of the Cayley Graph $X(SL(2, \mathbb{Z}/157\mathbb{Z}), \{t, t^{-1}, w, w^{-1}\})$, excluding the first and second largest eigenvalues, setting

$$t = \begin{pmatrix} 14 & 144 \\ 101 & 153 \end{pmatrix} \quad and \quad w = \begin{pmatrix} 114 & 129 \\ 140 & 124 \end{pmatrix},$$

looks extremely close to the Poisson cumulative distribution $1 - e^{-x}$.

4.1. Finite Euclidean Space. Along with some colleagues at U.C.S.D. we have looked at histograms of various Cayley graphs. Some of this is discussed in more detail in my book [**82**]. In the following discussion p is always an odd prime to make life simpler. We begin with finite analogues of Euclidean space.

We want to replace real symmetric spaces such as the plane $\mathbb{R}^2$ with finite analogues like $\mathbb{F}_p^2$, where $\mathbb{F}_p$ denotes the field with p elements. We can define a finite "distance" on vectors $x = \begin{pmatrix} x_1 \\ x_2 \end{pmatrix} \in \mathbb{F}_p^2$ by

$$d(x, y) = (x_1 - y_1)^2 + (x_2 - y_2)^2. \tag{4.2}$$

This distance is not a metric but it is invariant under translation and a finite analogue of rotation and thus under a finite analogue of the Euclidean motion group.

Define the **finite Euclidean plane graph** to be the Cayley graph $X(\mathbb{F}_p^2, S)$, where $S = S(a, p)$ consists of solutions $x = (x_1, x_2) \in \mathbb{F}_p^2$ of the congruence

$$x_1^2 + x_2^2 \equiv a \,(mod\, p).$$

The points in S form a finite circle. It turns out (Exercise 4) that the eigenvalues of the adjacency matrices for these graphs are essentially **Kloosterman sums**, for column vectors $b \in \mathbb{F}_p^2$:

$$\lambda_b = \sum_{x \in S} e^{2\pi i {}^t bx/p}. \tag{4.3}$$

Here ${}^t b$ =transpose of b and thus ${}^t bx = b_1x_1 + b_2x_2$. Kloosterman sums are finite analogues of Bessel functions just as Gauss sums are finite analogues of gamma functions. See Terras [**82**]. pp. 76, 90.

EXERCISE 4. *Prove that for odd primes p the eigenvalues in (4.3) are given by*

$$\lambda_{2c} = \frac{G_1^2}{p} K(a, d(c, 0)),$$

where $d(x, y)$ is as in (4.2), G_1 is the ***Gauss sum***

$$G_1 = \sum_{t=0}^{p-1} \varepsilon(t) e^{2\pi i t/p},$$

*with $\varepsilon(t) = \left(\frac{t}{p}\right) =$ **the Legendre symbol**; i.e.,*

$$\varepsilon(t) = \begin{cases} 0, & \text{if } p \text{ divides } t \\ 1, & \text{if } t \text{ is a square mod } p \\ -1, & \text{otherwise.} \end{cases}$$

Finally the ***Kloosterman sum*** *is*

$$K(a, b) = \sum_{t=1}^{p-1} \exp\left(\frac{2\pi i(at + b/t)}{p}\right). \tag{4.4}$$

See p. 95 of my book [**82**] *for hints.*

André Weil ([**90**], Vol. I, pp. 386-9) estimated the Kloosterman sum (4.4) which implies that the finite Euclidean graphs are Ramanujan when $p \equiv 3 (mod\ 4)$. In the case $p \equiv 1 (mod\ 4)$, the graphs may fail to be exactly Ramanujan but they are asymptotically Ramanujan as $p \longrightarrow \infty$. Katz [**43**] has proved that the distribution of the Kloosterman sums becomes semi-circle in the limit for large p. The top part of Figure 7 gives the histogram for the spectrum of one of the finite Euclidean plane graphs. The bottom part of Figure 7 gives the level spacing for the same Cayley graph, which does indeed look to be Poisson.

However when one replaces the 2-dimensional Euclidean graphs with three-dimensional analogues, the Kloosterman sums can be evaluated as sines or cosines. If we throw out the half of the eigenvalues of $E_{48611}(3, 1)$ that are 0, we obtain the histogram in the top of Figure 8 which is definitely not the semi-circle distribution. If we had kept the 0 eigenvalues, there would also be a peak at the origin. The normalized level spacing histogram for $E_{48611}(3, 1)$ is in the bottom of Figure 8. And the bottom does not appear to be Poisson either. See Terras [**82**] for more information. Bannai et al [**7**] have generalized these Euclidean graphs to association schemes for finite orthogonal groups.

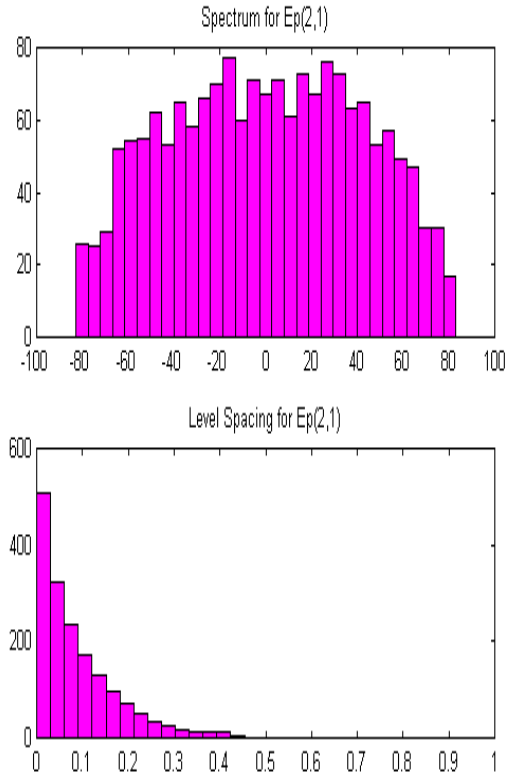

FIGURE 7. The top histogram is the spectrum (without multiplicity) of the adjacency matrix of the finite Euclidean plane graph $X(\mathbb{F}_p^2, S)$, where $p = 1723$ and S consists of solutions to the congruence $x_1^2 + x_2^2 \equiv 1\,(mod\, p)$.The bottom is the unnormalized level spacing histogram for the same graph.

The finite Euclidean graphs can be Ramanujan or not depending on their mood. For example, in 3 dimensions as in Figure 8, one finds that the graphs are not Ramanujan when the prime $p \equiv 3 (\mathrm{mod}\, 4)$ is larger than 158. The 3 dimensional graphs as in Figure 8 are always Ramanujan when $p \equiv 1 (\mathrm{mod}\, 4)$ In the 2-dimensional case as in Figure 7, one finds that the graphs are always Ramanujan if $p \equiv 3 (\mathrm{mod}\, 4)$ When $p \equiv 1 (\mathrm{mod}\, 4)$, on the other hand, sometimes the graphs are not Ramanujan; e.g., when p=17 and 53. The list of primes for which these graphs are not Ramanujan is a bit mysterious at this point. See Bannai et al [**7**].

4.2. Finite Upper Half Planes. We can replace the finite Euclidean plane $\mathbb{F}_q^2$ with the **finite non-Euclidean "upper" half plane** $H_q \subset \mathbb{F}_q(\sqrt{\delta})$ where δ is a non-square in the finite field $\mathbb{F}_q$ (for q odd) and

$$H_q = \left\{ z = x + y\sqrt{\delta} \mid x, y \in \mathbb{F}_q, \;\; y \neq 0 \right\}.$$

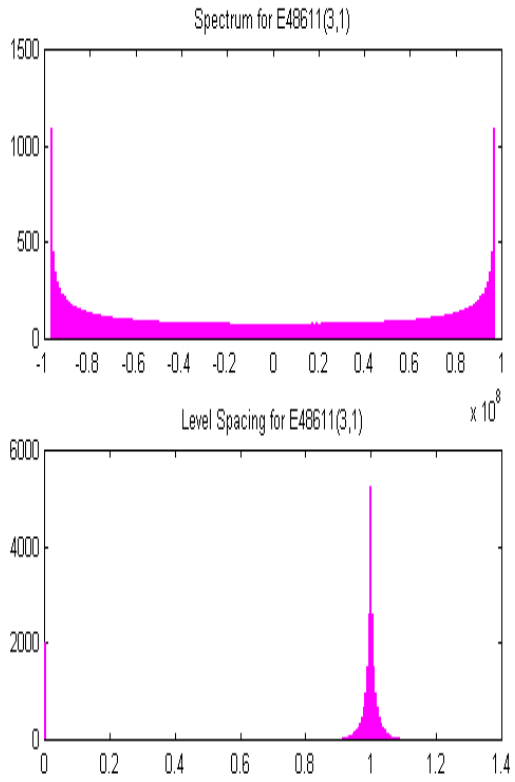

FIGURE 8. The top histogram is that of the spectrum (without multiplicity) of the adjacency matrix of the finite Euclidean 3-space graph $X(\mathbb{F}_p^3, S)$, where $p = 48611$ and S consists of solutions to the congruence $x_1^2 + x_2^2 + x_3^2 \equiv 1 \, (mod\, p)$. The bottom histogram is the normalized level spacing histogram for the same graph.

Our finite analogue of the complex numbers is $\mathbb{F}_q(\sqrt{\delta}) = \mathbb{F}_{q^2}$. We have all the usual algebraic rules for computing in the field of complex numbers. For example, define, for $z = x + y\sqrt{\delta}$, the imaginary part of z to be $y = Im(z)$. And define the conjugate $\overline{z} = x - y\sqrt{\delta}$, the norm $Nz = z\overline{z}$.

We define a **non-Euclidean "distance"** by

$$d(z, w) = \frac{N(z - w)}{Im(z)Im(w)}. \tag{4.5}$$

This is a natural finite analogue of the Poincaré metric for the classical hyperbolic upper half plane. See Lecture 2 or Terras [**82**], [**83**]. For example $d(z, w)$ is invariant under fractional linear transformation

$$z \longrightarrow \frac{az + b}{cz + d}, \quad \text{with} \quad \begin{pmatrix} a & b \\ c & d \end{pmatrix} \in G = GL(2, \mathbb{F}_q) \quad \text{meaning that} \quad ad - bc \neq 0.$$

Fix an element $a \in \mathbb{F}_q$ with $a \neq 0, 4\delta$. Define the vertices of the **finite upper half plane graph** $P_q(\delta, a)$ to be the elements of H_q. Connect vertex z to vertex w iff $d(z, w) = a$. See the Figure 14 in Lecture 2 for examples of such graphs.

EXERCISE 5. *Show that the octahedron is the finite upper half plane graph* $P_3(-1, 1)$.

It turns out (see Terras [**82**]) that simultaneous eigenfunctions for the adjacency matrices of these graphs, for fixed δ as a varies over $\mathbb{F}_q$, are spherical functions for the symmetric space G/K, where K is the subgroup fixing $\sqrt{\delta}$. Thus K is a finite analogue of the group of real rotation matrices $O(2, \mathbb{R})$. We will say more about symmetric spaces in the last section of this set of lectures. In particular, see Table 2 in Lecture 2 for a comparison of spherical functions on our 3 favorite symmetric spaces.

A **spherical function** (see [**82**], Chapter 20) $h : G \longrightarrow \mathbb{C}$ is defined to be a K bi-invariant eigenfunction of all the convolution operators by K- bi-invariant functions; it is normalized to have the value 1 at the identity. Here K- bi-invariant means $f(kxh) = f(x)$, for all $k, h \in K, x \in G$ and **convolution** means $f * h$, where

$$(f * h)(x) = \sum_{y \in G} f(y) h(y^{-1}x). \tag{4.6}$$

These are generalizations of Laplace spherical harmonics (see Terras [**83**], Vol. I, Chapter 2). Equivalently h is a spherical function means h is an eigenfunction for the adjacency matrices of all the graphs $P_q(\delta, a)$, as a varies over $\mathbb{F}_q$. One can show ([**82**], p. 347) that any **spherical function** has the form

$$h(x) = \frac{1}{|K|} \sum_{k \in K} \chi(kx), \text{ where } \chi \text{ is a character of } G = GL(2, \mathbb{F}_q). \tag{4.7}$$

Here χ is an irreducible character appearing in the induced representation of the trivial representation of K induced up to G. In this situation (when G/K is a symmetric space or (G, K) a Gelfand pair) **eigenvalues = eigenfunctions**. See Stanton [**72**] and Terras [**82**], p. 344. Thus our eigenvalues are finite analogues of Legendre polynomials.

One can also view the eigenvalues of the finite upper half plane graphs as entries in the character table of an association scheme. See Bannai [**6**]. And this whole subject can be reinterpreted in the language of Hecke algebras. See Krieg [**47**].

Soto-Andrade [**71**] managed to rewrite the sum (4.7) for the case $G/K \cong H_q$ as an explicit exponential sum which is easy to compute (see [**82**], p. 355 and Ch. 21). Thus we can call the eigenvalues of the finite upper half plane graphs **Soto-Andrade sums**. Katz [**42**] estimated these sums to show that the finite upper half plane graphs are indeed Ramanujan. Winnie Li [**49**] gives a different proof.

The spectral histograms for the finite upper half plane graphs for fairly large q look like Figure 9. The spectra appear to resemble the semi-circle distribution and the level spacings appear to be Poisson. Recently Ching-Li Chai and Wen-Ching Winnie Li [**18**] have proved that the spectra of finite upper half plane graphs do approach the semi-circle distribution as q goes to infinity. They use the Jacquet-Langlands correspondence for $GL(2)$ over function fields and the connection Winnie Li has made between the finite upper half plane graphs and Morgenstern's function field analogues (see [**61**]) of the Lubotzky, Phillips and Sarnak graphs. See Li's article in [**37**] pp. 387-403. Note that the result of Chai and Li does not follow

from the work of McKay [**58**] because the degrees of the finite upper half plane graphs approach infinity with q. The Poisson behavior of the level spacings for finite upper half planes is still only conjectural.

However if you replace the finite field $\mathbb{F}_q$ with a finite ring like $\mathbb{Z}/q\mathbb{Z}$, for $q = p^r$, p =prime, $r > 1$, the spectral histograms change to those in Figure 10 which do not resemble the semi-circle at all.

Here we view finite upper half planes as providing a "toy" symmetric space. But an application has been found (see Tiu and Wallace [**88**]).

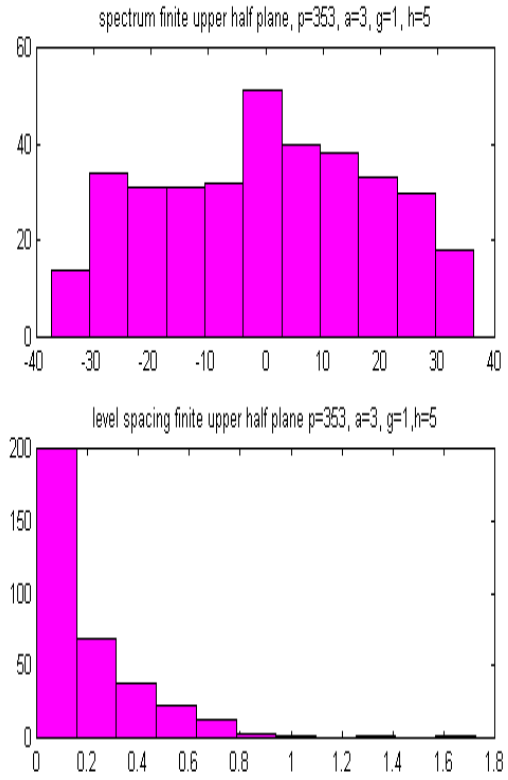

FIGURE 9. Histograms of Spectra of Finite Upper Half Plane Graphs (without multiplicity) $P_{353}(3, 3)$. In our program to compute Soto-Andrade sums we needed to know that a generator of the multiplicative group of $\mathbb{F}_{353}(\sqrt{3})$ is $1 + 5\sqrt{3}$. The top histogram is for the spectrum and the lower one is for the unnormalized level spacing.

EXERCISE 6. *Define finite upper half plane graphs over the finite fields of characteristic 2. The spectra of these graphs have been considered in Angel* [**3**] *and Evans* [**27**]. *Using a result of Katz, the non-trivial graphs have also been proved to be Ramanujan.*

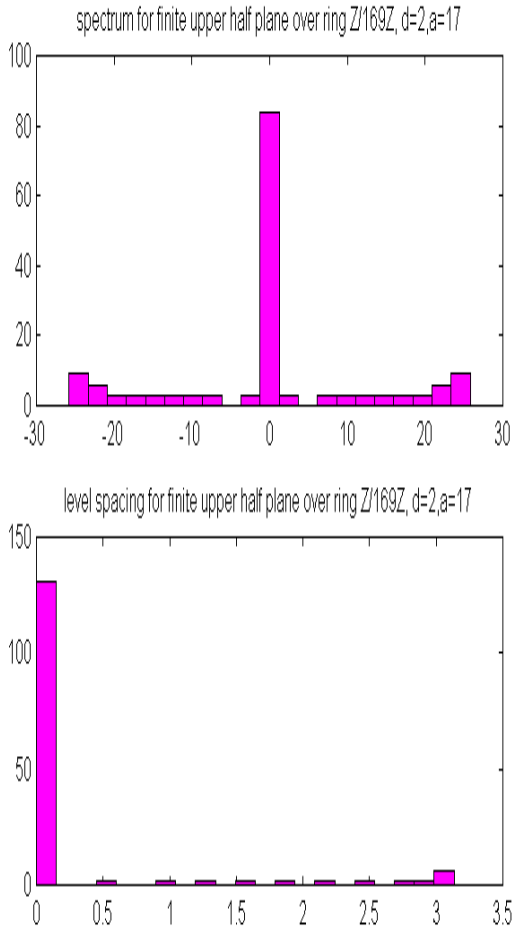

FIGURE 10. Histograms of Spectra (without multiplicity) of Finite Upper Half Plane Graphs over the Ring $\mathbb{Z}/169\mathbb{Z}$ with $d = 2$ and $a = 17$. The top histogram is that for the spectrum and the bottom one is that for the unnormalized level spacing. Data was computed by B. Shook using Matlab. See Angel et al [**4**].

4.3. Dreams of "Larger" Groups and Butterflies. What happens if you consider "larger" matrix groups such as $GL(3, F)$? What happens if you replace graphs with hypergraphs or buildings? Do new phenomena appear in the spectra? See Fan Chung's article in Friedman [**31**] as well as K. Feng and Winnie Li [**28**] and Li and P. Solé [**51**] for hypergraphs. In [**56**] María Martínez constructs some hypergraphs analogues of the symmetric space for $GL(n, \mathbb{F}_q)$ using n-point invariants and shows that some of these hypergraphs are Ramanujan in the sense of Feng and Li. See also [**57**]. Recently Cristina Ballantine [**5**] and Winnie Li [**50**] have found an analogue of the Lubotzky, Phillips and Sarnak examples of Ramanujan

graphs for $GL(n)$ using the theory of buildings, which are higher dimensional analogues of trees. See also the Ph.D. thesis of Alireza Sarveniazi at the Universität Göttingen. Nancy Allen [**2**] and F. J. Marquez [**55**] have considered Cayley graphs for 3x3-matrix analogues of the affine group of matrices $\begin{pmatrix} y & x \\ 0 & 1 \end{pmatrix}$, with distances analogous to that for the finite upper half plane graphs.

An important subgroup of $GL(3)$ corresponding to the s-coordinates in the finite upper half plane is the **Heisenberg group** $H(F)$ over a ring or field F. $H(F)$ consists of matrices $\begin{pmatrix} 1 & x & z \\ 0 & 1 & y \\ 0 & 0 & 1 \end{pmatrix}$, with $x, y, z \in F$. When F is the field of real numbers, this group is important in quantum physics, in particular, when considering the uncertainty principle. It is also important in signal processing, in particular, for the theory of radar. See Terras [**82**], Chapter 18. When the ring $F = \mathbb{Z}$, the ring of integers, there are degree 4 and 6 infinite Cayley graphs associated to $H(\mathbb{Z})$ whose spectra have been much studied, starting with D. R. Hofstadter's work on energy levels of Bloch electrons, which includes a diagram known as Hofstadter's butterfly. This subject also goes under the name of the spectrum of the almost Mathieu operator or the Harper operator. Or one can just consider the finite difference equation corresponding to Matthieu's differential equation $y'' - 2\theta\cos(2x)y = -ay$. M. P. Lamoureux's website (www.math.ucalgary.ca/~mikel/mathieu.html) has a picture and references. For results on the Cantor-set like structure of the spectrum, see M. D. Choi, G. A. Elliott, and Noriko Yui [**19**]. Other references are Béguin, Valette, and Zuk [**9**] or Motoko Kotani and T. Sunada [**46**].

In Terras [**82**], Chapter 18, you can find the representations of $H(\mathbb{F}_q)$, along with some applications. The analogue with the finite field $\mathbb{F}_q$ replaced with a finite ring $\mathbb{Z}/q\mathbb{Z}$ is in [**24**] along with applications to the spectra of Cayley graphs for the **Heisenberg group** $H(\mathbb{Z}/q\mathbb{Z})$. One generating set that we considered is the 4 element set $S = \{A, A^{-1}, B, B^{-1}\}$, when $AB \neq BA \pmod p$. When p is an odd prime all such graphs are isomorphic. When $p = 2$ there are only 2 isomorphism classes of these graphs. The histogram for the spectrum of the adjacency matrix for $p^n = 64$ is given in Figure 11 below. All the eigenvalue histograms we have produced for these degree 4 Heisenberg graphs look the same. Perhaps this is not surprising because setting $X_n = X(H(\mathbb{Z}/p^n\mathbb{Z}), \{A, A^{-1}, B, B^{-1}\})$ then X_{n+1} covers X_n. This implies, for example, that the spectrum of the adjacency operator on X_n is contained in that for X_{n+1}. See Stark and Terras [**73**].

M. Minei [**60**] has noticed that one can draw very different pictures of the spectra (see Hofstadter's butterfly in Figure 12) for these graphs by using Hofstadter's idea which leads to separating the spectra corresponding to the q-dimensional representations of the Heisenberg group $H(\mathbb{Z}/q\mathbb{Z})$. We defined these representations π_r, $r = 1, ..., q-1$ in [**24**]. Plot the part of the spectrum of the Cayley graph corresponding to π_r as points in the plane with y-coordinate $\frac{r}{q}$ and x-coordinates given by the eigenvalues λ of the matrix

$$M_r = \sum_{s \in S} \pi_r(s).$$

Of course λ must lie in the interval $[-4, 4]$. Hofstadter was interested in matrices analogous to those from graphs for the Heisenberg group over $\mathbb{Z}$ itself which is the limiting picture.

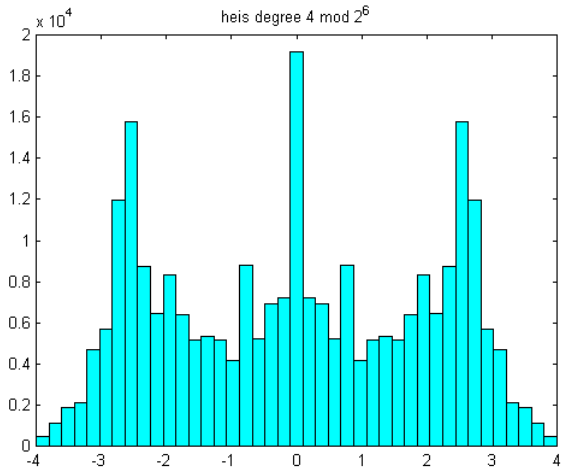

FIGURE 11. Histogram of the Eigenvalues of the Adjacency Operator for the degree 4 Cayley Graph of the Heisenberg group $Heis(64)$.

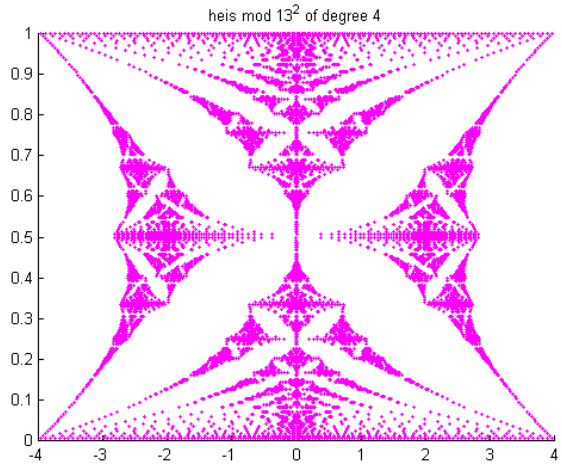

FIGURE 12. Hofstadter's Butterfly for the Highest Dimensional Part of the Spectrum of the Cayley Graph $H(169)$. The figure is obtained as described in the text.

The moral of Figure 12 is that there could be more useful ways of representing spectra than just histograms. But one needs a certain structure of the representations of the symmetry group in order to be able to see butterflies.

Part 2

Lecture 2. Three Symmetric Spaces

5. Zeta Functions of Graphs

First let us consider the graph theoretic analogue of Selberg's zeta function. This function was first considered by Ihara [**40**] in a paper that considers p-adic groups rather than graphs. Then Serre [**70**] explained the connection with graphs. Later authors extended Ihara's results to non-regular graphs and zeta functions of many variables. References are Bass [**8**], Hashimoto [**34**], Stark and Terras [**73**], [**74**], [**75**], [**76**], Sunada [**80**], Venkov and Nikitin [**89**].

Let X be a connected finite (not necessarily regular) graph with undirected edge set E. For examples look at Figure 14. We orient the edges of X arbitrarily and label them $e_1, e_2, ..., e_{|E|}, e_{|E|+1} = e_1^{-1}, ..., e_{2|E|} = e_{|E|}^{-1}$. Here the inverse of an edge is the edge taken with the opposite orientation. A **prime** $[C]$ in X is an equivalence class of tailless backtrackless primitive paths in X. Here write $C = a_1 a_2 \cdots a_s$, where a_j is an oriented edge of X. The **length** $\nu(C) = s$. **Backtrackless** means that $a_{i+1} \neq a_i^{-1}$, for all i. **Tailless** means that $a_s \neq a_1^{-1}$. The **equivalence class** of C is $[C] = \{a_1 a_2 \cdots a_s \ , \ a_2 \cdots a_s a_1 \ , ..., \ a_s a_1 a_2 \cdots a_{s-1}\}$; i.e., the same path with all possible starting points. We call the equivalence class **primitive** if $C \neq D^m$, for all integers $m \geq 2$, and all paths D in X.

DEFINITION 1. *The **Ihara zeta function** of X is defined for $u \in \mathbb{C}$ with $|u|$ sufficiently small by*

$$\zeta_X(u) = \prod_{\substack{[C] \ prime \\ in \ X}} (1 - u^{\nu(C)})^{-1}.$$

THEOREM 1. *(Ihara). If A denotes the adjacency matrix of X and Q the diagonal matrix with jth entry q_j = (degree of the jth vertex - 1), then*

$$\zeta_X(u)^{-1} = (1 - u^2)^{r-1} \det(I - Au + Qu^2).$$

Here r denotes the rank of the fundamental group of X. That is, $r = |E| - |V| + 1$.

For regular graphs, when $Q = qI$ is a scalar matrix, you can prove this theorem using the Selberg trace formula (discussed below) for the $(q+1)$-regular tree T. See Terras [**82**] or Venkov and Nikitin [**89**]. Here $X = T/\Gamma$, where Γ denotes the fundamental group of X. In the general case there are many proofs. See Stark and Terras [**73**], [**74**] for some elementary ones. A survey with lots of references is to be found in Hurt [**39**].

Example. The Ihara zeta function of the tetrahedron.

$$\zeta_{K_4}(u)^{-1} = (1 - u^2)^2 (1 - u)(1 - 2u)(1 + u + 2u^2)^3.$$

EXERCISE 7. *a) For a regular graph show that $r - 1 = |V|(q-1)/2$, where $|V|$ is the number of vertices, r is the rank of the fundamental group, $q+1$ is the degree.*

b) Compute the Ihara zeta function of the finite upper half plane graph over the field with 3 elements.

c) For a $(q+1)$-regular graph, find a functional equation relating the values $\zeta_X(u)$ and $\zeta_X(1/(qu))$.

Note that since the Ihara zeta function is the reciprocal of a polynomial, it has no zeros. Thus when discussing the Riemann hypothesis we consider only poles. When X is a finite connected $(q+1)$-regular graph, there are many analogues of

the facts about the other zeta functions. For any unramified graph covering Y of X (not necessarily normal, or even involving regular graphs) it is easy to show that the reciprocal of the zeta function of X divides that of Y (see Stark and Terras [**73**]). The analogue of this for Dedekind zeta functions of extensions of number fields is still unproved. Analogously to the Dedekind zeta function of a number field, special values of the Ihara zeta function give graph theoretic constants such as the number of spanning trees. See Exercise 8. There is also an analogue of the Chebotarev density theorem (see Hashimoto [**35**]).

EXERCISE 8. *Show that defining the "complexity" of the graph* $\kappa(X)$ = *the number of spanning trees of* X, *we have the formula*

$$(-1)^{r+1} r 2^r \kappa(X) = \frac{d^r (\zeta_X)^{-1}}{du^r}(1).$$

There are hints on the last page of [**82**].

When X is a finite connected $(q+1)$-regular graph, we say that $\zeta_X(q^{-s})$ **satisfies the Riemann hypothesis** iff

$$for\ \ 0 < \operatorname{Re} s < 1, \quad \zeta_X(q^{-s})^{-1} = 0 \Longleftrightarrow \operatorname{Re} s = \frac{1}{2}. \tag{5.1}$$

EXERCISE 9. *Show that the Riemann hypothesis (5.1) is equivalent to saying that* X *is a* ***Ramanujan graph*** *in the sense of Lubotzky, Phillips, and Sarnak* [**53**]. *This means that when* λ *is an eigenvalue of the adjacency matrix of* X *such that* $|\lambda| \neq q+1$, *then* $|\lambda| \leq 2\sqrt{q}$.

REMARK 2. *Lubotzky* [**54**] *has defined what it means for a finite irregular graph* Y *covered by an infinite graph* X *to be* X*-Ramanujan. It would be useful to reinterpret this in terms of the poles of the Ihara zeta function of the graph. It would also be nice to know if there is a functional equation for the Ihara zeta of an irregular graph.*

Table 1 below is a zoo of zetas, comparing three types of zeta functions: number field zetas (or Dedekind zetas), zetas for function fields over finite fields, and finally the Ihara zeta function of a graph. Thus it adds a new column to Table 2 in Katz and Sarnak [**45**]. In Table 1 it is assumed that our graphs are finite, connected and regular. Here "GUE" means that the spacing between pairs of zeros/poles is that of the eigenvalues of a random Hermitian matrix. Columns 1-3 are essentially taken from Katz and Sarnak. Column 4 is ours. One should also make a column for Selberg zeta and L-functions of Riemannian manifolds. We have omitted the last row of the Katz and Sarnak table. It concerns the monodromy or symmetry group of the family of zeta functions. See Katz and Sarnak [**44**] for an explanation of that row.

Hashimoto [**34**], p. 255, shows that the congruence zeta function of the modular curve $X_0(\ell)$ over a finite field $\mathbb{F}_p$ is essentially the Ihara zeta function of a certain graph X attached to the curve. And he finds that the number of $\mathbb{F}_p$ rational points of the Jacobian variety of $X_0(\ell)$ is the class number of the function field of the modular curve ($p \neq \ell$) and is related to the complexity of X. Thus in some cases our 4th column is the same as the function field zeta column in [**45**].

type of ζ or L-function	number field	function field	(regular) graph theoretic
functional equation	yes	yes	yes, many
spectral interpretation of 0's/poles	?	yes	yes
RH	expect it	yes	iff graph Ramanujan
level spacing of high zeros/poles GUE	expect it	yes for almost all curves	?

Table 1. The Zoo of Zetas - A New Column for Table 2 in Katz and Sarnak [**45**].

6. Comparisons of the Three Types of Symmetric Spaces

We arrange our comparisons of symmetric spaces G/K in a series of figures and tables. The goal is to compare the Selberg trace formula in the 3 spaces. Figure 13 shows the three spaces with the Poincaré upper half plane on the upper left, the 3-regular tree on bottom, and the finite upper half space over the field with 3 elements on the upper right. Of course, we cannot draw all of the infinite spaces H and T. In Table 2, the first column belongs to the Poincaré upper half plane, the second column to the $(q+1)$-regular tree, the third column to the finite upper half plane over $\mathbb{F}_q$. Note that we split the table into two parts, with part 1 containing the first 2 columns and part 2 containing the 3rd column. Here $\mathbb{F}_q$ denotes a finite field with an odd number q of elements. Table 2 can be viewed as a dictionary for the 3 languages.

Symmetric spaces G/K can be described in terms of Gelfand pairs (G, K) of group G and subgroup K. This means that the convolution algebra of functions on G which are K bi-invariant is a commutative algebra. Here **convolution** of functions $f, g : G \longrightarrow \mathbb{C}$ is given by formula (4.6) for discrete G Replace the sum in (4.6) by an integral with respect to Haar measure on continuous G

For the Poincaré upper half plane the group G is the special linear group $SL(2, \mathbb{R})$ which consists of 2×2 real matrices of determinant 1 acting on H by fractional linear transformation. In the case of the finite upper half plane the group is the general linear group $G = GL(2, \mathbb{F}_q)$ which consists of 2×2 matrices with entries in the finite field and non-0 determinant.

For the second column, we will emphasize the graph theory rather than the group theory as that would involve p-adic groups which would require more background of the reader and not even include the most general degree graphs. See Li [**49**] or Nagoshi [**63**] for the p-adic point of view. Thus for the $(q+1)$-regular tree we view the group G as a group of graph automorphisms, meaning 1-1, onto maps from T to T preserving adjacency. There are 3 types of such automorphisms of T. See Figá-Talamanca and Nebbia [**29**] for a proof.

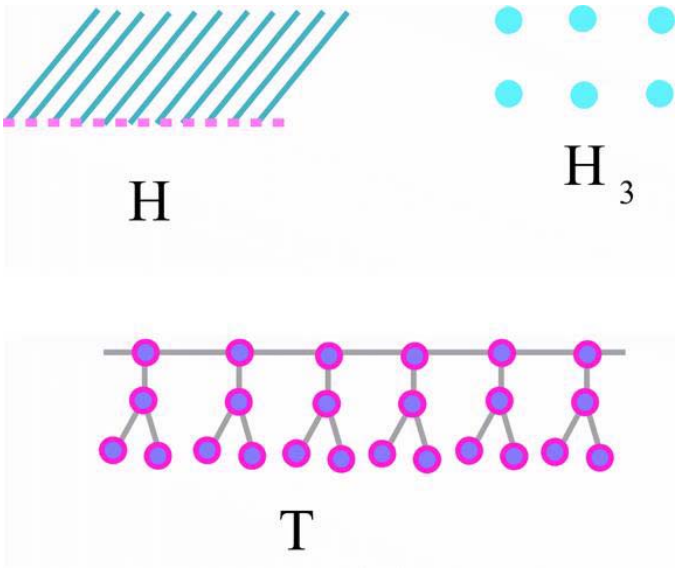

FIGURE 13. The 3 Symmetric Spaces. The Poincaré upper half plane H is on the upper left. The 3-regular tree T is on the bottom, and the finite upper half plane H_3 over the field with 3 elements is on the upper right.

AUTOMORPHISMS OF THE TREE T

- rotations fix a vertex;
- inversions fix an edge and exchange endpoints;
- hyperbolic elements ρ fix a geodesic $\{x_n | n \in \mathbb{Z}\}$ and $\rho(x_n) = x_{n+s}$. That is, ρ shifts along the geodesic by $s = \nu(\rho)$. We define "geodesic" below. One is pictured in Figure 15.

The subgroup K of $g \in G = SL(2, \mathbb{R})$ such that $gi = i$ is easily seen to be the special orthogonal group $SO(2, \mathbb{R})$ of 2×2 rotation matrices. The analogue for $G = GL(2, \mathbb{F}_q)$ consists of elements fixing the origin $\sqrt{\delta}$ in the finite upper half plane H_q and it is the subgroup K of matrices of the form $k_{a,b} = \begin{pmatrix} a & b\delta \\ b & a \end{pmatrix}$. It is easily seen that the map sending $k_{a,b}$ to $a + b\sqrt{\delta}$ provides a group isomorphism from K to the multiplicative group of $\mathbb{F}_q(\sqrt{\delta})$.

In Figure 14 we show the finite upper half plane graph for $q = 3$ (the octahedron) and one of the 3 different finite upper half plane graphs for $q = 5$ (drawn on a dodecahedron).

In Figures 15 and 16, we illustrate some of the geometry of the symmetric spaces. **Geodesics** in the Poincaré upper half plane are curves which minimize the Poincaré distance ds from Table 2. It is not hard to see that the points in H on the y-axis form a geodesic and thus so do the images of this curve under fractional linear transformations from $G = SL(2, \mathbb{R})$ since ds is G-invariant. These are semicircles and half-lines orthogonal to the real axis. These are the straight lines of a non-Euclidean geometry.

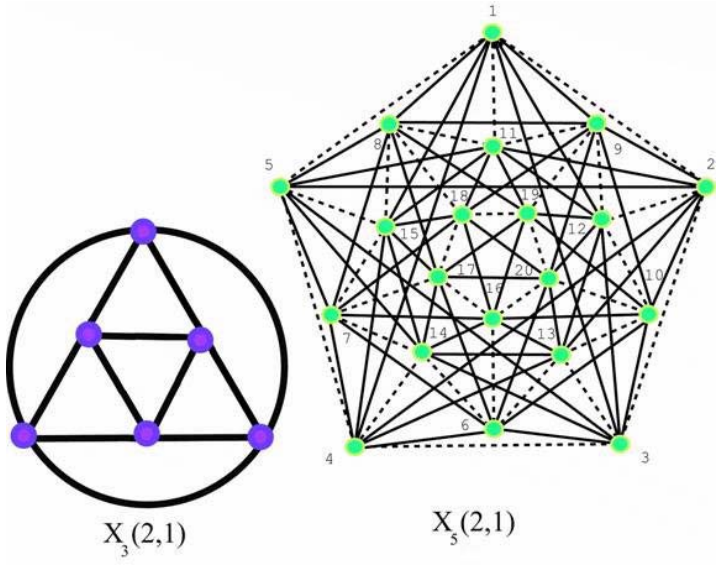

FIGURE 14. Some finite upper half plane graphs for $q = 3$ and 5. The graph for $q = 5$ is shown on a dodecahedron whose edges are indicated by dotted lines while the edges of the graph $X_5(2, 1)$ are given by solid lines.

Geodesics in the tree are paths $\{x_n \,|\, n \in \mathbb{Z}\}$ which are infinite in both directions (i.e., x_n is connected to x_{n+1} by an edge). We define **geodesics** in the finite upper half plane to be images of the analogue of the y-axis under fractional linear transformation by elements of $GL(2, \mathbb{F}_q)$. The three types of geodesics are illustrated in Figure 15.

Horocycles are curves orthogonal to the geodesics. The horocycles are pictured in Figure 16. In the Poincaré upper half plane they are lines parallel to the x-axis and their images by fractional linear transformation from $SL(2, \mathbb{R})$. For the finite upper half plane we make the analogous definition of horocycles.

In the tree, horocycles are obtained by fixing a half geodesic or chain $C = [\mathcal{O}, \infty] = \{x_n \mid n \in \mathbb{Z},\ n \geq 0\}$. Then the chain connecting a point x in the tree to infinity along C is called $[x, \infty]$. If x and y are points of T, then $[x, \infty] \cap [y, \infty] = [z, \infty]$. We say x and y are equivalent if $d(x, z) = d(y, z)$. Horocycles with respect to C are the equivalence classes for this equivalence relation.

Next we consider **spherical functions** on the symmetric spaces. These are K-invariant eigenfunctions of the Laplacian(s) which are normalized to have the value 1 at the origin. Since the power function $y^s = \mathrm{Im}(z)^s$ is an eigenfunction of the Laplacian on H corresponding to the eigenvalue $s(s-1)$, we can build up spherical functions from the power function by integration over K. Here dk denotes the Haar measure given by $d\theta$, if $k = \begin{pmatrix} \cos\theta & \sin\theta \\ -\sin\theta & \cos\theta \end{pmatrix}$. See Terras [**83**] for more information on spherical functions for continuous symmetric spaces.

A similar method works for the tree except that the analogue of the power function $p_s(x) = q^{-sd(x,\mathcal{O})}$ is not quite an eigenfunction for the adjacency operator

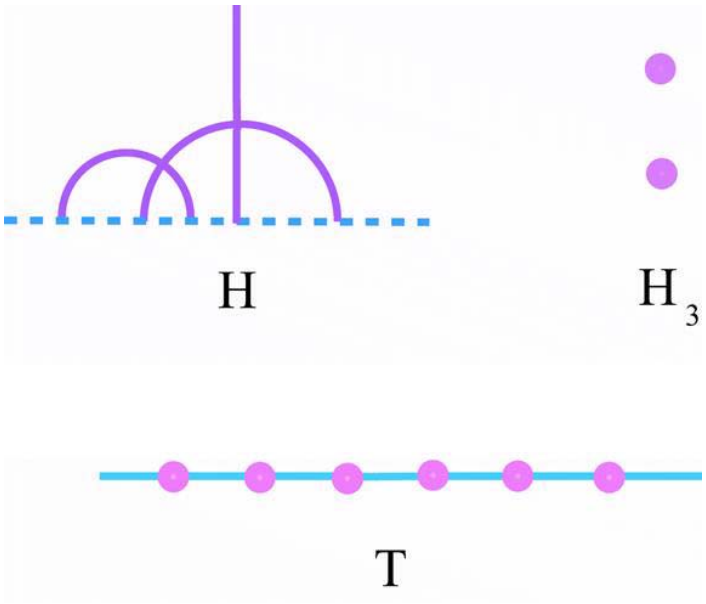

FIGURE 15. Geodesics in the 3 Symmetric Spaces H, T, and H_3.

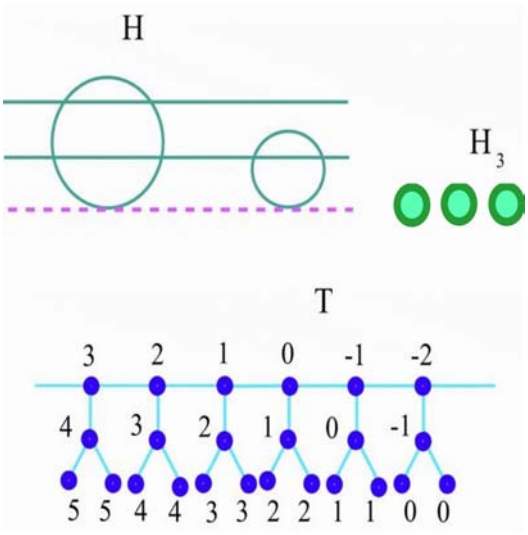

FIGURE 16. Horocycles in the 3 Symmetric Spaces H, T, and H_3. For the tree, points in the nth horocycle are labeled n.

on T with eigenvalue $\lambda = q^s + q^{1-s}$. This is fixed by writing $h_s(x) = c(s)p_s(x) + c(1-s)p_{1-s}(x)$, with

$$c(s) = \frac{q^{s-1} - q^{1-s}}{(q+1)(q^{s-1} - q^{-s})}, \quad \text{if} \quad q^{2s-1} \neq 1. \tag{6.1}$$

Take limits when $q^{2s-1} = 1$. More information on spherical functions on trees can be found in references [**15**], [**17**], [**29**], [**82**], [**87**].

For the finite upper half plane one can build up spherical functions from characters of inequivalent irreducible unitary representations π of $G = GL(2, \mathbb{F}_q)$ occurring in the left regular representation of G on functions in $L^2(G/K)$. This is the same thing as saying that π occurs in the induced representation $Ind_K^G 1$. See Terras [**82**], Ch. 16, for the definition of induced representation. We use $\widehat{G}^K$ to denote the set of π occurring in $Ind_K^G 1$. Then the spherical function h_π corresponding to π is obtained by averaging the character $\chi_\pi = Trace(\pi)$ over K as in formula (4.7) in Lecture 1. See Terras [**82**] for more information on these finite spherical functions and the representations of $GL(2, \mathbb{F}_q)$.

The **spherical transform** of a function f in $L^2(K\backslash G/K)$; i.e., a K-bi-invariant function on G, is obtained by integrating (summing) f times the spherical function over the symmetric space G/K. These transforms are invertible in all 3 cases.

Poincaré Upper Half Plane	$(q+1)$**-regular Tree**
space $= H =$ $\{z = x + iy \mid x, y \in \mathbb{R}, y > 0\}$	**space** $= T =$ $(q+1)$-regular connected graph with no circuits
group $G = SL(2,\mathbb{R})$ $\left\{ \begin{pmatrix} a & b \\ c & d \end{pmatrix} \middle\vert\, ad - bc = 1 \right\}$	**group** $G =$ graph automorphisms of T rotations, inversions, shifts
group action $gz = \frac{az+b}{cz+d}$, $z \in H$	**group action** gx
origin $= i$	**origin** = any point $\mathcal{O}$
subgroup K fixing origin $SO(2,\mathbb{R}) = \{g \in G \vert^t gg = I\}$	**subgroup** K fixing origin rotations about $\mathcal{O}$
$\mathbf{H \cong G/K}$	$\mathbf{T \cong G/K}$
arc length $ds^2 = \frac{dx^2+dy^2}{y^2}$	**graph distance**=# edges in path joining 2 points $x, y \in T$
Laplacian $\Delta = y^2 \left(\frac{\partial}{\partial x^2} + \frac{\partial}{\partial y^2} \right)$	$\Delta = A - (q+1)I$, A=**adjacency operator** for T
spherical function $h_s(z) = \int_K (\mathrm{Im}(ka))^s dk$, $\Delta h_s = s(s-1)h_s$	**spherical function** $p_s(x) = q^{-sd(x,\mathcal{O})}$, with $c(s)$ as in (6.1) $h_s(x) = c(s)p_s(x) + c(1-s)p_{1-s}(x)$
spherical transform of $f : K\backslash G/K \longrightarrow \mathbb{C}$ $\widehat{f}(s) = \int_H f(z)\overline{h_s(z)}\frac{dxdy}{y^2}$	**spherical transform** of $f : K\backslash G/K \longrightarrow \mathbb{C}$ $\widehat{f}(s) = \sum_{x \in T} f(x)\overline{h_s(x)}$
inversion $f(z) =$ $\frac{1}{4\pi} \int_{\mathbb{R}} \widehat{f}(\frac{1}{2} + it) h_{\frac{1}{2}+it}(z) t \tanh \pi t \; dt$	**inversion** $f(x) =$ $\int_{-2\sqrt{q}}^{2\sqrt{q}} \widehat{f}(\frac{1}{2} + it) h_{\frac{1}{2}+it}(x) \frac{\sqrt{4q-t^2}}{(q+1)^2 - t^2} dt$
horocycle transform $F(y) = y^{-1/2} \int_{\mathbb{R}} f(x+iy)dx$ invertible	**horocycle transform** $\mathfrak{h} =$ horocycle on T $F(\mathfrak{h}) = \sum_{x \in \mathfrak{h}} f(x)$ invertible

Table 2. Part 1. Basic geometry of the Poincaré upper half plane and the (q+1)-regular tree.

Finite Upper Half Plane
space $= H_q =$ $\{z = x + \sqrt{\delta}y \mid x, y \in \mathbb{F}_q, y \neq 0\}$ where $\delta \neq a^2$, for any $a \in \mathbb{F}_q$
group $G = GL(2, \mathbb{F}_q)$ $\left\{ \begin{pmatrix} a & b \\ c & d \end{pmatrix} \middle\vert\, ad - bc \neq 0 \right\}$
group action $gz = \frac{az+b}{cz+d}$, $z \in H_q$
origin $= \sqrt{\delta}$
subgroup K fixing origin $=$ $K = \left\{ \begin{pmatrix} a & b\delta \\ b & a \end{pmatrix} \in G \right\} \cong \mathbb{F}_q(\sqrt{\delta})^*$
$\mathbf{H \cong G/K}$
pseudo-distance $d(z, w) = \frac{N(z-w)}{\operatorname{Im} z \operatorname{Im} w}$, $Im(x + y\sqrt{\delta}) = y, Nz = (x^2 - y^2\delta)$
$X_a = X_q(\delta, a)$, **graph** - vertices $z \in H_q$ edge between z and w if $d(z, w) = a$ $\Delta = A_a - (q+1)I$, if $a \neq 0$ or 4δ $A_a =$ **adjacency operator** for X_a
spherical function $h_\pi(z) = \frac{1}{\lvert K \rvert} \sum_K \chi_\pi(kz)$, $\pi \in \widehat{G}^K$, *i.e.*, π occurs in $Ind_K^G 1, d_\pi = \deg \pi$
spherical transform of $f : K\backslash G/K \longrightarrow \mathbb{C}$ $\widehat{f}(\pi) = \sum_{z \in H_q} f(z)\overline{h_\pi(z)}$
inversion $f(z) = \frac{1}{\lvert G \rvert} \sum_{\pi \in \widehat{G}^K} d_\pi \widehat{f}(\pi) h_\pi(z)$
horocycle transform $F(y) = \sum_{x \in \mathbf{F}_q} f(x + y\sqrt{\delta})$ not invertible

Table 2. Part 2. Basic geometry of the finite upper half plane.

The **horocycle transform** of f is obtained by integrating or summing f over a horocycle in the symmetric space. These horocycle transforms are invertible in 2 out of 3 cases.

The **Selberg trace formula** involves another subgroup Γ of G. This subgroup should be discrete and for ease of discussion have compact quotient $\Gamma\backslash G/K$. For $G = SL(2, \mathbb{R})$, this sadly rules out the modular group $\Gamma = SL(2, \mathbb{Z})$. For examples of such $\Gamma \subset SL(2, \mathbb{R})$, see Svetlana Katok's book [**41**]. In Table 3 we give a dictionary of trace formulas for the 3 types of symmetric spaces considered here.

Fundamental domains D for $\Gamma\backslash G/K$ in the various symmetric spaces G/K are depicted in Figure 17. Interactive fundamental domain drawers can be found on Helena Verrill's webpage (http:hverrill.net).

Tessellations of G/K by the action of copies of these fundamental domains are quite beautiful. Instead of drawing tessellations in Figures 18, 19, 20 we

give contour maps of various functions. Tessellations of H by the modular group given by contour maps of modular forms are to be found on Frank Faris's website (ricci.scu.edu/~ffaris).

Γ **discrete subgroup** of G	$\Gamma \subset G$, fundamental group of X
with $\Gamma\backslash H$ compact, no fixed points	$X = \Gamma\backslash T$ finite $(q+1)$-regular connected graph
conjugacy classes in Γ $\{\gamma\} = \{x\gamma x^{-1} \vert x \in \Gamma\}$	**conjugacy classes** in Γ
center $\{\pm I\}$	**identity**
hyperbolic $\gamma \backsim \pm \begin{pmatrix} t & 0 \\ 0 & t^{-1} \end{pmatrix}$, $t > 1, t \neq t^{-1}$ **centralizer** $\Gamma_\gamma = \{x \in \Gamma \vert x\gamma = \gamma x\}$ =cyclic$=<\gamma_0>$ γ_0 **primitive hyperbolic**	**hyperbolic** γ fixes geodesic C shifts along C by $\nu(\gamma)$ $\Gamma_\gamma = \{x \in \Gamma \vert x\gamma = \gamma x\}$ $=<\gamma_0>$ γ_0 **primitive hyperbolic**
Spectrum Δ on $L^2(\Gamma\backslash G/K)$ $\Delta\varphi_n = \lambda_n\varphi_n,\ \ n = 0, 1, 2, ...,$ $\lambda_n = s_n(1 - s_n) \leq 0$	$A\varphi_n = \lambda_n\varphi_n,\ \lambda_n = q^{s_n} + q^{1-s_n}$ $\vert\lambda_n\vert \neq q+1 \Longrightarrow 0 < \mathrm{Re}\,(s_n) < 1$ X Ramanujan $\Longleftrightarrow$ for $\vert\lambda_n\vert \neq q+1, \mathrm{Re}\,(s_n) = \frac{1}{2}$
Selberg trace formula $\sum_{\lambda_n = s_n(1-s_n)} \widehat{f}(s_n) = area(\Gamma\backslash H) f(i)$ $+ \sum_{\{\gamma\}\ hyperbolic} \frac{\log N\gamma_0}{N\gamma^{\frac{1}{2}} - N\gamma^{-\frac{1}{2}}} F(N\gamma)$	**Selberg trace formula** $f(x) = f(d(x, \mathcal{O}))$ $\sum_{i=1}^{\vert X\vert} \widehat{f}(s_i) = f(0)\vert X\vert$ $+ \sum_{\{\rho\}\ hyperbolic} \nu(\rho) \sum_{e \geq 1} Hf(e\nu(\rho))$ $F(\mathfrak{h}_n) = c_n Hf(n),$ $c_n = \begin{cases} 2^n, n > 0 \\ 1, n \leq 0 \end{cases}$ $Hf(n) = f(\vert n\vert)$ $+(q-1) \sum_{j \geq 1} q^{j-1} f(\vert n\vert + 2j)$
Selberg zeta function $Z(s) = \prod_{\{\gamma_0\}} \prod_{j \geq 0} (1 - N\gamma_0^{-s-j})$ non-trivial zeros correspond to spectrum Δ on $L^2(\Gamma\backslash G/K)$ except for finite # of zeros Riemann Hypothesis (R.H.) $s \in (0,1), \mathrm{Re}(s) = \frac{1}{2}$	**Ihara zeta function** $\zeta_X(s) = \prod_{\{\rho_0\}} (1 - u^{\nu(\rho)})^{-1},\ \ u = q^{-s}$ $\zeta_X(s)^{-1} =$ $(1-u^2)^{r-1} \det(I - Au + qu^2 I)$ $r = rank\ \Gamma,\ r - 1 = \frac{\vert X\vert(q-1)}{2}$ $\zeta_X(s)$ satisfies R.H. $\Longleftrightarrow X$ is Ramanujan

Table 3. Part 1. Trace formulas for the the continuous and discrete symmetric spaces.

$\Gamma \subset G$; $\Gamma = GL(2, \mathbb{F}_p)$
conjugacy classes in Γ
central $\begin{pmatrix} a & 0 \\ 0 & a \end{pmatrix}, a \in \mathbb{F}_p^*$
hyperbolic $\begin{pmatrix} a & 0 \\ 0 & b \end{pmatrix}$, $a \neq b \in \mathbb{F}_p^*$
parabolic $\begin{pmatrix} a & 1 \\ 0 & a \end{pmatrix}, a \in \mathbb{F}_p^*$
elliptic $\begin{pmatrix} a & b\xi \\ b & a \end{pmatrix}$ $a, b \in \mathbb{F}_p, b \neq 0,$ $\xi \neq u^2$, $u \in \mathbb{F}_p$
Selberg trace formula $(\mathbf{q} = \mathbf{p}^2)$ $\sum_{\pi \in \widehat{G}^K} \widehat{f}(\pi) mult(\pi, Ind_\Gamma^G 1)$ $= \lvert\Gamma\backslash G\rvert(p-1)f(\sqrt{\delta})$ $+\frac{(q+1)(q-1)^2}{2(p-1)} \sum_{\substack{c \in F_p^* \\ c \neq 1}} F(c)$ $+\frac{q(q^2-1)}{p}\{F(1) - F(\sqrt{\delta})\}$ $+\frac{q^2-1}{2} \sum_{\substack{a,b \in \mathbb{F}_p \\ b \neq 0}} F(\frac{a+b\eta}{a-b\eta})$, where $\eta^2 = \xi$, $\eta \in \mathbb{F}_q$
Unknown if there is an analogue of Selberg zeta function

Table 3. Part 2. Trace formula for the the finite symmetric spaces.

In column 1 of Table 3, note that there are only two types of conjugacy classes in Γ. The hyperbolic conjugacy classes $\{\gamma\}$ correspond to γ with diagonal Jordan form with distinct diagonal entries t and $1/t$ having $t > 1$. The norm of such an element is $N\gamma = t^2$. The centralizer Γ_γ of γ is a cyclic group with generator the primitive hyperbolic element γ_0. The numbers $logN\gamma_0$ represent lengths of closed geodesics in the fundamental domain $\Gamma\backslash H$. The set of these numbers is the "length spectrum". The length spectrum can be viewed as analogous to the set of primes in $\mathbb{Z}$.

The spectrum of the Laplacian on the fundamental domain $\Gamma\backslash H$ consists of a sequence of negative numbers λ_n with $|\lambda_n| \longrightarrow \infty$. And $\lambda_0 = 0$ corresponds to the constant eigenfunction. We write $\lambda_n = s_n(1 - s_n)$. The eigenfunction φ_n corresponding to λ_n is called a cuspidal **Maass wave form**. They are much like classical holomorphic automorphic forms. The Selberg trace formula given in Table 3 column 1 involves the spherical transform of a function f in $L^2(K\backslash G/K)$ as well as the horocycle transform of f. Since there are only two types of conjugacy classes in Γ when the fundamental domain is compact and Γ acts without fixed points, there are only two sorts of terms on the right-hand side of the formula. For a Γ like $SL(2,\mathbb{Z})$ there will also be elliptic and parabolic conjugacy classes.

The Selberg trace formula provides a correspondence between the length spectrum and the Laplacian spectrum. It thus gives analogues of many of the explicit formulas in analytic number theory. There are many applications; e.g. to prove the Weyl law for the number of $|\lambda_n| \leq x$ as $x \longrightarrow \infty$. The **Weyl law** says

$$\#\{\lambda_n \mid |\lambda_n| \leq x\} \sim \frac{area(\Gamma\backslash H)x}{4\pi}, \text{as } x \to \infty.$$

The Weyl law implies that cuspidal Maass wave forms exist when $\Gamma\backslash H$ is compact. This can also be proved when Γ is arithmetic. See Terras [**83**], for more information. In general it has been conjectured by Sarnak that such cuspidal Maass wave forms need not exist.

One can also deduce the prime geodesic theorem from the trace formula. Here we only mention the application to the Selberg zeta function defined in Table 3. The trace formula can be used to show that the Selberg zeta function has many of the properties of the Riemann zeta function and moreover for it one has the Riemann hypothesis saying that its non-trivial zeros are on the line $Re\,(s) = \frac{1}{2}$.

Column 2 of Table 3 gives the graph theoretic analogue of all of this. Here Γ is the fundamental group of the finite connected $(q+1)$-regular graph $X = \Gamma\backslash T$. And the tree T is the universal covering graph of X. The non-central conjugacy classes in Γ are hyperbolic. Again the hyperbolic γ fixes a geodesic in T and operates by shifting along the geodesic by $\nu(\gamma)$

The spectrum of the adjacency operator on X consists of eigenvalues $\lambda_n = q^{s_n} + q^{1-s_n}$. If $|\lambda_n| \neq q+1$, then $0 < Re\,(s_n) < 1$. Recall that the graph X is defined by Lubotzky, Phillips and Sarnak [**53**] to be Ramanujan if $|\lambda_n| \neq q+1 \Longrightarrow |\lambda_n| \leq 2\sqrt{q}$. This is equivalent to saying $\mathrm{Re}(s_n) = \frac{1}{2}$ by Exercise 9.

Again the Selberg trace formula in the second column of Table 3 involves the spherical transform of a function f in $L^2(\Gamma\backslash T)$ as well as the horocycle transform. These transforms are defined in Table 2. The Selberg trace formula for the first two columns of Table 3 has only two sorts of terms because again there are only two sorts of conjugacy classes in Γ - central and hyperbolic. The table gives the relationship between the horocycle transform defined in the last rows of Table 2 and that appearing in the trace formula for trees.

Once more, there is an application to zeta functions. In this case it is the Ihara zeta function of the finite graph X. That function was defined at the beginning of this lecture and in column 2 of Table 3 as a product over primitive hyperbolic elements of Γ. This product can also be viewed as one over closed primitive backtrackless, tailless paths in X. The trace formula gives an explicit formula for the function as the reciprocal of a polynomial. There are also direct combinatorial proofs of this fact that work more generally for irregular graphs. This suggests that

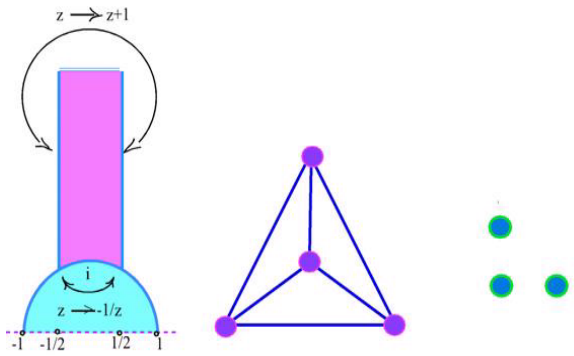

FIGURE 17. Fundamental domains for some discrete subgroups. That for $SL(2,\mathbb{Z})\backslash H$ is on the left. That for the 3-regular tree mod the fundamental group of K_4 is in the center. That for $SL(2,\mathbb{F}3)\backslash H_9$ is on the right.

there exists some more general version of the Selberg trace formula for irregular graphs.

It is possible to use this work to prove the graph theoretic analogue of the prime number/geodesic theorem among other things. See Terras and Wallace [**87**]. Another proof comes from theorem 1. For this theorem yields an exact formula relating prime cycles in X and poles of the Ihara zeta function.

Finally, column 3 of Table 3 concerns the trace formula for finite upper half planes. Here it is not clear what sort of subgroups Γ one should consider. We look mainly at the case $G = GL(2,\mathbb{F}_q)$ and $\Gamma = GL(2,\mathbb{F}_p)$, where $q = p^r$. There are 4 types of conjugacy classes $\{\gamma\}$ in Γ, according to the Jordan form of γ. These are listed in the third column of Table 3. Then we give the trace formula only in the case that $q = p^2$. The general case can be found in Terras [**82**].

Once more the left hand side of the trace formula is a sum of spherical transforms of f this time over representations appearing in the induced representation $Ind_\Gamma^G 1$. The right hand side involves horocycle transforms of f and now there are 4 types of terms because there are 4 types of conjugacy classes. The parabolic terms are not so hard to deal with as in the continuous case since there can be no divergent integrals. The elliptic terms are a bit annoying because they behave differently depending on whether q is an even or odd power of p.

We could not fill in the last rows of the third column of table 3 because we have not found an analogue of the Selberg zeta function for finite upper half plane graphs. We have worked out a number of examples of the formula in [**82**].

One might question our definition of elliptic and hyperbolic here. In the classical case of $SL(2,\mathbb{R})$, hyperbolic means eigenvalues real and distinct while elliptic means eigenvalues complex.

Next we consider $\Gamma-$**Tessellations of the 3 Symmetric spaces**. The first (in Figure 18) is that of the Poincaré upper half plane given by using Mathematica to give us a density plot of y^6 times the absolute value of the cusp form of weight 12 known as $\Delta(x+iy)$, the discriminant. The next (in Figure 19) is the tessellation

of the 3-regular tree obtained by defining a function which has values 1,2,3,4 on the 4 vertices of K_4. The last (in Figure 20) is a density plot for an $SL(2, \mathbb{F}_7)$ invariant function on H_{49}.

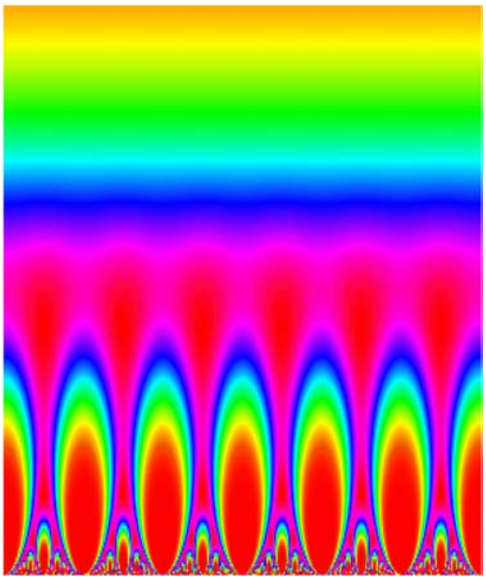

FIGURE 18. Tessellation of the Poincaré upper half plane corresponding to the absolute value of the modular form delta times y^6

EXERCISE 10. *a) Make columns for Tables 2 and 3 for the Euclidean spaces* $\mathbb{R}^n$ *and* $\mathbb{F}_q^n$.
b) Draw the Euclidean analogues of Figures 13-17.

EXERCISE 11. *Compute the fundamental domain for* $GL(2, \mathbb{F}_5)$ *acting on* H_{25}.

EXERCISE 12. *Show that if* $Z(u)$ *is the Selberg zeta function in column 1 of Table 3, then* $Z(s+1)/Z(s)$ *has the same sort of product formula as the Ihara zeta function in column 2 of the same table.*

If you would like to read more about trace formulas on continuous symmetric spaces, some references are: Buser [**16**], Elstrodt [**25**], Elstrodt, Grunewald and Mennicke [**26**], Hejhal [**36**], Selberg [**69**] and Terras [**83**]. References for the trace formula on trees are: Ahumada [**1**], Nagoshi [**63**], Terras [**82**] and Venkov and Nikitin [**89**]. A reference for the trace formula on finite upper half planes is Terras [**82**].

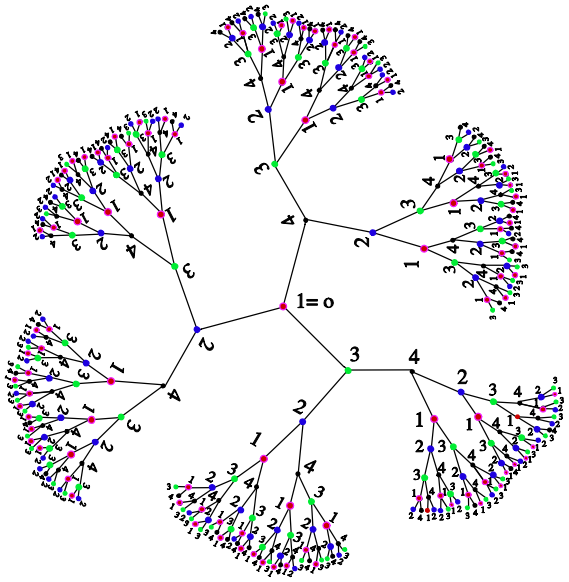

FIGURE 19. Tessellation of the 3-regular tree from K_4

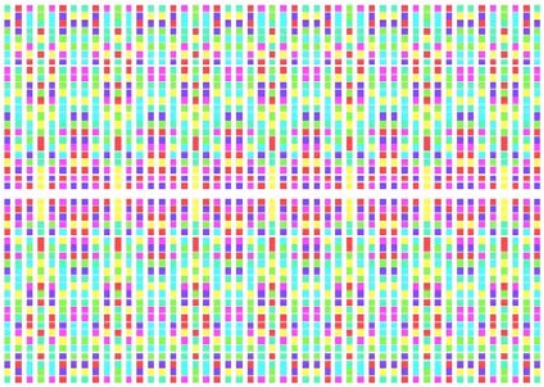

FIGURE 20. Tessellation of H_{49} from $GL(2, \mathbb{F}_7)$

7. Pictures of Eigenfunctions

We will make only a few remarks here about the studies quantum chaoticists make of eigenfunctions of their favorite operators. The main problem here concerns the behavior of level curves of eigenfunctions. This question is a mathematical analogue of physicists' questions. The nodal lines $(\varphi_n = 0)$ can be seen by putting dust on a vibrating drum. One question quantum physicists ask is: Do the nodal lines of eigenfunctions φ_n "scar" (accumulate) on geodesics as the eigenvalue approaches infinity? The answer in the arithmetical quantum chaotic situation appears to be "No" thanks to work of Sarnak et al [**67**]. You can see

FIGURE 21. Arithmetical quantum chaos for the modular group - the topography of Maass wave forms for the modular group from Dennis Hejhal http://www.math.umn.edu/~hejhal

this in the pictures of eigenfunctions of the Laplacian for Maass wave forms. Figure 21 is a representative picture from an older version of D. Hejhal's website (http://www.math.umn.edu/~hejhal/). Note that the scarring in Figure 18 is along horocycles.

Figures 22 and 23 give the finite Euclidean and non-Euclidean analogues. Animations of the contour maps of Figures 22 and 23, as p grows, are to be found at my website

http://math.ucsd.edu/~aterras/euclid.gif

and http://math.ucsd.edu/~aterras/chaos.gif.

In Figure 22, the level curves are finite analogues of circles. They look like Fresnel diffraction patterns. See Goetgheluck for a discussion. Of course, there is no real reason to stick to our favorite finite analogue of Euclidean distance. Perla Myers [**62**] has considered finite Euclidean graphs with more general distances, for which the "level curves" also give quite beautiful figures. See also Bannai et al [**7**]. Figure 23 should be compared with Figure 21.

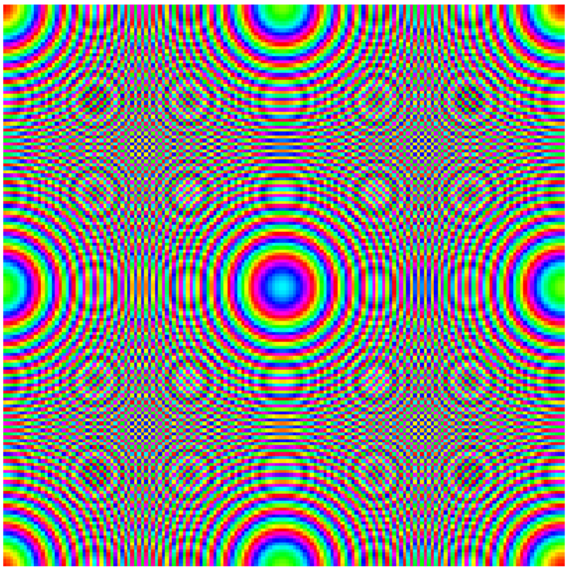

FIGURE 22. Level "curves" for eigenfunctions of the adjacency matrix for finite Euclidean space with $p = 163$.

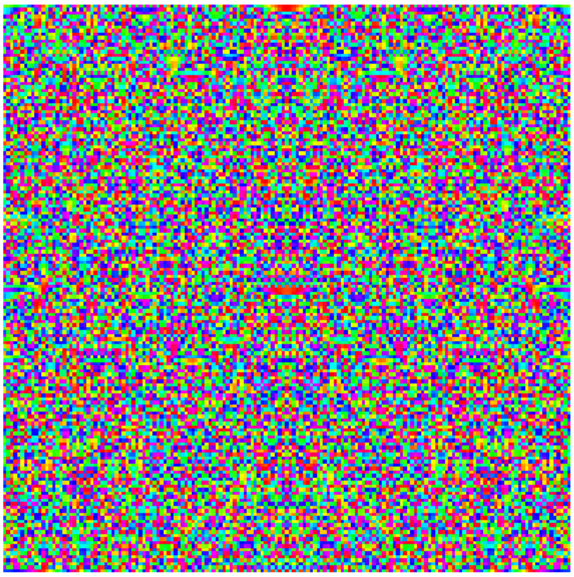

FIGURE 23. Level "curves" for eigenfunctions of the adjacency matrix for the finite upper half plane mod 163.

Bibliography

[1] G. Ahumada, *Fonctions periodiques et formule des traces de Selberg sur les arbres*, C. R. Acad. Sci. Paris, **305** (1987), 709-712.

[2] N. Allen, *On the spectra of certain graphs arising from finite fields*, Finite Fields Applics., **4** (1998), 393-440.

[3] J. Angel, *Finite upper half planes over finite fields*, Finite Fields Applics., **2** (1996), 62-86.

[4] J. Angel, B. Shook, A. Terras, C. Trimble, *Graph spectra for finite upper half planes over rings*, Linear Algebra and its Applications, **226-228** (1995), 423-457.

[5] C. Ballantine, *Ramanujan type buildings*, Canad. J. Math., **52** (2000), 1121-1148.

[6] E. Bannai, *Character tables of commutative association schemes*, in Finite Geometries, Buildings, and Related Topics, (W. M. Kantor, et al, Eds.), Clarendon Press, Oxford, 1990, pp. 105-128.

[7] E. Bannai, O. Shimabukuro, and H. Tanaka, *Finite euclidean graphs and Ramanujan graphs*, preprint.

[8] H. Bass, *The Ihara-Selberg zeta function of a tree lattice*, Internatl. J. Math., **3** (1992), 717-797.

[9] C. Béguin, A. Valette, and A. Zuk, *On the spectrum of a random walk on the discrete Heisenberg group and the norm of Harper's operator*, J. of Geometry and Physics, **21** (1997), 337-356.

[10] N. Biggs, *Algebraic Graph Theory*, Cambridge U. Press, Cambridge, 1974.

[11] O. Bohigas and M.-J. Giannoni, *Chaotic motion and random matrix theories*, Lecture Notes in Physics, **209**, Springer-Verlag, Berlin, 1984, pp. 1-99.

[12] O. Bohigas, R.U. Haq, and A. Pandey, *Fluctuation properties of nuclear energy levels and widths: comparison of theory with experiment*, in K.H. Böckhoff (Ed.), Nuclear Data for Science and Technology, Reidel, Dordrecht, 1983, pp. 809-813.

[13] B. Bollobas, *Modern Graph Theory*, Springer-Verlag, N.Y., 1998.

[14] A. Borel and G. D. Mostow, *Algebraic Groups and Discontinuous Subgroups*, Proc. Symp. Pure Math., **IX**, Amer. Math. Soc., Providence, 1966.

[15] R. Brooks, *The spectral geometry of k-regular graphs*, J. d'Analyse, **57** (1991), 120-151.

[16] P. Buser, *Geometry and Spectra of Compact Riemann Surfaces*, Birkhäuser, Boston, 1992.

[17] P. Cartier, *Harmonic analysis on trees*, Proc. Symp. Pure Math., **26**, Amer. Math. Soc., Providence, 1973, pp. 419-423.

[18] C.-L. Chai and W.-C. W. Li, *Character sums and automorphic forms*, preprint.

[19] M. D. Choi, G.A. Elliott, and N. Yui, *Gauss polynomials and the rotation algebra*, Inventiones Math., **99** (1990), 225-246.

[20] F. R. Chung, *Spectral Graph Theory*, Amer. Math. Soc., Providence, 1997.

[21] F. Chung and S. Sternberg, *Mathematics and the buckyball*, American Scientist, **81** (1993), 56-71.

[22] B. Cipra, *What's Happening in the Mathematical Sciences, 1998-1999*, Amer. Math. Soc., Providence, RI, 1999.

[23] D.M. Cvetković, M. Doob, and H. Sachs, *Spectra of Graphs: Theory and Application*, Academic, N.Y., 1979.

[24] M. DeDeo, M. Martinez, A. Medrano, M. Minei, H. Stark, and A. Terras, *Spectra of Heisenberg graphs over finite rings: histograms, zeta functions and butterflies*, preprint (on the web at http://math.ucsd.edu/~aterras/heis.pdf).

[25] J. Elstrodt, *Die Selbergsche Spurformel für kompakte Riemannsche Flächen*, Jber. d. Dt. Math.-Verein., **83** (1981), 45-77.

[26] J. Elstrodt, F. Grunewald, and J. Mennicke, *Groups acting on Hyperbolic Space*, Springer-Verlag, Berlin, 1998.
[27] R. Evans, *Spherical functions for finite upper half planes with characteristic 2*, Finite Fields Applics, **3** (1995), 376-394.
[28] K. Feng and W. Li, *Spectra of hypergraphs and applications*, J. Number Theory, **60** (1996), 1-22.
[29] A. Figá-Talamanca and C. Nebbia, *Harmonic Analysis and Representation Theory for Groups acting on Homogeneous Trees*, Cambridge U. Press, Cambridge, 1991.
[30] P. J. Forrester and A. Odlyzko, *A nonlinear equation and its application to nearest neighbor spacings for zeros of the zeta function and eigenvalues of random matrices*, in Proceedings of the Organic Math. Workshop, Invited Articles, located at http://www.cecm.sfu.ca/~pborwein/
[31] J. Friedman (Ed.), *Expanding Graphs*, DIMACS Series in Disc. Math. and Th. Comp. Sci., **10**, Amer. Math. Soc., Providence, 1993.
[32] P. Goetgheluck, *Fresnel zones on the screen*, Experimental Math., **2** (1993), 301-309.
[33] F. Haake, *Quantum Signatures of Chaos*, Springer-Verlag, Berlin, 1992.
[34] K. Hashimoto, *Zeta functions of finite graphs and representations of p-adic groups*, Adv. Stud. Pure Math., **15**, Academic, N.Y., 1989, pp. 211-280.
[35] K. Hashimoto, *Artin-type L-functions and the density theorem for prime cycles on finite graphs*, Internatl. J. Math., **3** (1992), 809-826.
[36] D. A. Hejhal, *The Selberg trace formula and the Riemann zeta function*, Duke Math. J., **43** (1976), 441-482.
[37] D.A. Hejhal, J. Friedman, M.C. Gutzwiller and A. M. Odlyzko (Eds.), Emerging Applications of Number Theory, IMA Volumes in Math. and its Applications, **109**, Springer-Verlag, N.Y., 1999.
[38] D. R. Hofstadter, *Energy levels and wave functions of Bloch electrons in rational and irrational magnetic fields*, Phys. Rev. B, **14** (1976), 2239-2249.
[39] N. Hurt, *Finite volume graphs, Selberg conjectures, and mesoscopic systems: A review*, preprint, 1998.
[40] Y. Ihara, *On discrete subgroups of the two by two projective linear group over a p-adic field*, J. Math. Soc. Japan,**18** (1966), 219-235.
[41] S. Katok, *Fuchsian Groups*, Univ. of Chicago Press, Chicago, 1992.
[42] N. Katz, *Estimates for Soto-Andrade sums*, J. Reine Angew. Math., **438** (1993), 143-161.
[43] N. Katz, *Gauss Sums, Kloosterman Sums, and Monodromy Groups*, Princeton Univ. Press, Princeton, N.J., 1988.
[44] N. Katz and P. Sarnak, *Random Matrices, Frobenius Eigenvalues and Monodromy*, Amer. Math. Soc., Providence, RI, 1999.
[45] N. Katz and P. Sarnak, *Zeroes of zeta functions and symmetry*, Bull. Amer. Math. Soc., **36**, No. 1 (1999), 1-26.
[46] M. Kotani and T. Sunada, *Spectral geometry of crystal lattices*, preprint.
[47] A. Krieg, *Hecke Algebras*, Memoirs of Amer. Math. Soc., **435**, Providence, 1990.
[48] J.D. Lafferty and D. Rockmore, *Fast Fourier analysis for SL_2 over a finite field and related numerical experiments*, Experimental Math., **1** (1992), 115-139.
[49] W. Li, *Number Theory with Applications*, World Scientific, Singapore, 1996.
[50] W. Li, *Ramanujan graphs and Ramanujan hypergraphs*, Park City Lectures, 2002.
[51] W. Li and P. Solé, *Spectra of regular graphs and hypergraphs and orthogonal polynomials*, Europ. J. Combinatorics, **17** (1996), 461-477.
[52] A. Lubotzky, *Discrete Groups, Expanding Graphs, and Invariant Measures*, Birkhäuser, Boston, 1994.
[53] A. Lubotzky, R. Phillips, and P. Sarnak, *Ramanujan graphs*, Combinatorica, **8** (1988), 261-277.
[54] A. Lubotzky, *Cayley graphs, eigenvalues, expanders and random walks*, Surveys in Combinatorics, 1995, Ed. P. Rowlinson, Cambridge U. Press, Cambridge, 1995, pp. 155-189.
[55] F. J. Marquez, *Ph. D. thesis*, U.C.S.D., 2000.
[56] M. G. Martínez, *The finite upper half space and related hypergraphs*, J. Number Theory, **84** (2000), 342-360.
[57] M. G. Martínez, H. M. Stark, and A. Terras, *Some Ramanujan hypergraphs associated to $GL(n, \mathbb{F}_q)$*, Proc. Amer. Math. Soc., **129** (2000), 1623-1629.

[58] B. McKay, *The expected eigenvalue distribution of a large regular graph*, J. Lin. Alg. Appl., **40** (1981), 203-216.
[59] M. L. Mehta, *Random Matrices and the Statistical Theory of Energy Levels*, Academic, N.Y., 1990.
[60] M. Minei, *Ph.D. Thesis*, U.C.S.D., 2000.
[61] M. Morgenstern, *Ramanujan diagrams*, S.I.A.M. J. Discrete Math., **7** (1994), 560-570.
[62] P. Myers, *Ph.D. Thesis*, U.C.S.D., 1995.
[63] H. Nagoshi, *On arithmetic infinite graphs*, Proc. Japan Acad., **76**, Ser. A (2000), 22-25.
[64] M. Rubinstein, *Evidence for a spectral interpretation of zeros of L-functions, Ph.D. Thesis*, Princeton, 1998.
[65] Z. Rudnick, *Some problems in "quantum chaos" or statistics of spectra*, Park City Lectures, 2002.
[66] P. Sarnak, *Some Applications of Modular Forms*, Cambridge U. Press, Cambridge, 1990.
[67] P. Sarnak, *Arithmetic quantum chaos*, Israel Math. Conf. Proc., **8** (1995), 183-236 (published by the Amer. Math. Soc.).
[68] C. Schmit, *Quantum and classical properties of some billiards on the hyperbolic plane*, in Chaos and Quantum Physics, Eds. M.- J. Giannoni et al, Elsevier, N.Y., 1991, pp. 333-369.
[69] A. Selberg, *Harmonic analysis and discontinuous groups in weakly symmetric Riemannian spaces with applications to Dirichlet series*, J. Ind. Math. Soc., **20** (1954), 47-87.
[70] J.-P. Serre, *Trees*, Springer-Verlag, N.Y., 1980.
[71] J. Soto-Andrade, *Geometrical Gel'fand models, tensor quotients, and Weil representations*, Proc. Symp. Pure Math., **47**, Amer. Math. Soc., Providence, 1987, pp. 305-316.
[72] D. Stanton, *An introduction to group representations and orthogonal polynomials*, Orthogonal Polynomials: Theory and Practice, Edited by P. Nevai and M. E. H. Ismail, Kluwer, Dordrecht, 1990, 419-433.
[73] H.M. Stark and A. Terras, *Zeta functions of finite graphs and coverings*, Advances in Math., **121** (1996), 124-165.
[74] H.M. Stark and A. Terras, *Zeta functions of finite graphs and coverings*, Part II, Advances in Math., **154** (2000), 132-195.
[75] H. M. Stark and A. Terras, *Artin L-functions of graph coverings,* Proceedings of the Conference on Dynamical, Spectral and Arithmetic Zeta Functions, Contemporary Math., **290** (2001), 181-195.
[76] H. M. Stark and A. Terras, *Zeta functions of graph coverings*, Proc. DIMACS Workshop on Unusual Applications of Number Theory, ed. Melvyn B. Nathanson, in press.
[77] M. E. Starzak, *Mathematical Methods in Chemistry and Physics*, Plenum, N.Y., 1989.
[78] S. Sternberg, *Group Theory and Physics*, Cambridge U. Press, Cambridge, 1994.
[79] A. Strömbergsson, *On the zeros of L-functions associated to Maass waveforms*, International Math. Res. Notices, **15** (1999), 839-851.
[80] T. Sunada, *Fundamental groups and Laplacians*, Lecture Notes in Math., **1339**, Springer-Verlag, N.Y., 1987, p. 248-277.
[81] A. Terras, *Survey of spectra of Laplacians on finite symmetric spaces*, Experimental Math., **5** (1996), 15-32.
[82] A. Terras, *Fourier Analysis on Finite Groups and Applications*, Cambridge Univ. Press, Cambridge, U.K., 1999.
[83] A. Terras, *Harmonic Analysis on Symmetric Spaces and Applications, I,II*, Springer-Verlag, N.Y., 1985, 1988.
[84] A. Terras, *Statistics of graph spectra for some finite matrix groups: Finite Quantum Chaos*, Proc. International Workshop on Special Functions, June, 1999, C. Dunkl et al, Eds., World Scientific, Singapore, 2000, pp. 351-374.
[85] A. Terras, *Comparison of Selberg's trace formula with its discrete analogues*, Proc. DIMACS Workshop on Unusual Applications of Number Theory, ed. Melvyn B. Nathanson, in press.
[86] A. Terras, *Finite Quantum Chaos*, American Math. Monthly, **109** (2002), 121-139.
[87] A. Terras and D. Wallace, *Selberg's Trace Formula on the k-Regular Tree and Applications*, International J. of Math. and Math. Sciences, **2003, No. 8** (Feb., 2003), 501-526.
[88] P. D. Tiu and D. Wallace, *Norm quadratic residue codes*, IEEE Trans. Inform. Theory, **40 (3)**, (1994), 946-949.
[89] A. B. Venkov and A. M. Nikitin, *The Selberg trace formula, Ramanujan graphs and some problems of mathematical physics*, Petersburg Math. J., **5 (3)**, (1994), 419-484.

[90] A. Weil, *Collected Papers*, Vols. I-III, Springer-Verlag, Berlin, 1979.
[91] E. P. Wigner, *Random matrices in physics*, S.I.A.M. Review, **9, No. 1** (1967), 1-23.